sustainability

MDPI

Article

Assessing Heat Stress in Lithuania Using Copernicus Data and National Heatwave Criteria

Inga Dailidienė [1,*], Aleksas Narščius [1,2], Beatričė Pargaliauskytė [1], Mathilde Raoux [3], Remigijus Dailidė [4], Rasa Grigoliene [5], Donatas Valiukas [6] and Laurynas Klimavičius [7]

[1] Marine Research Institute, Klaipeda University, LT-92294 Klaipeda, Lithuania
[2] Faculty of Technologies, Klaipeda State College, LT-91274 Klaipeda, Lithuania
[3] École Nationale de la Météorologie, Météo-France, 31100 Toulouse, France
[4] Faculty of Health Sciences, Klaipeda University, LT-92294 Klaipeda, Lithuania
[5] Faculty of Marine Technology and Natural Sciences, Klaipeda University, LT-92291 Klaipeda, Lithuania
[6] Lithuanian Hydrometeorological Service, LT-09300 Vilnius, Lithuania
[7] Department of Hydrology and Climatology, Institute of Geosciences, Vilnius University, LT-03225 Vilnius, Lithuania
* Correspondence: dailidiene.ku@gmail.com

Abstract

Climate warming is increasing heat-related risks and the need for sustainable adaptation across Europe, including Lithuania. This study assessed thermal stress in Lithuania during May–September over a 44-year period (1982–2025), using Copernicus ERA5 and ERA5-HEAT data alongside national meteorological station observations. Long-term changes in maximum air temperature (Tmax), the Universal Thermal Climate Index (UTCI), Humidex, and the frequency of hot days and tropical nights were examined. The comparison focused on Klaipėda, influenced by a maritime climate, and Vilnius, located approximately 300 km inland. The annual number of heat-stress days with moderate or greater heat stress (UTCI $\geq$ 26 °C) increased by 0.30 days per year in Klaipėda and 0.61 days per year in Vilnius, equivalent to approximately 3 and 6 additional days per decade, respectively. Increases were most pronounced in the moderate heat-stress category (26 °C $\leq$ UTCI $<$ 32 °C). Strong heat-stress days (32 °C $\leq$ UTCI $<$ 38 °C) were less frequent, with a slight increase observed only in Vilnius and rare occurrences in Klaipėda. Humidex also indicated increasing thermal discomfort at both locations. Although warm-season temperature percentiles were lower at the coast, tropical nights (minimum air temperature $\geq$ 20 °C) increased significantly in Klaipėda by 0.76 nights per decade ($p = 0.002$). A supplementary exploratory pilot spectral analysis identified indications of recurring Tmax variability at 2–3-year timescales, more pronounced in Klaipėda. These findings highlight the importance of assessing complementary daytime and nighttime heat indicators in maritime and continental settings.

Keywords: thermal stress; heatwaves; tropical nights; Universal Thermal Climate Index (UTCI); humidex; climate change adaptation; maritime–continental contrast

Check for updates

Academic Editor: Giouli Mihalakakou

Received: 23 September 2026
Revised: 29 October 2026
Accepted: 4 November 2026
Published: 7 November 2026

Copyright: © 2026 by the authors. Licensee MDPI, Basel, Switzerland. This article is an open access article distributed under the terms and conditions of the Creative Commons Attribution (CC BY) license.

1. Introduction

Climate change is increasing the frequency, intensity, and duration of warm-season temperature extremes [1], making heatwaves an increasingly important challenge for public health, urban planning, and climate adaptation. Their impacts are not determined by air temperature alone: human heat balance is also influenced by humidity, wind speed, short- and long-wave radiation, physical activity, clothing, acclimatisation, and the opportunity for nocturnal cooling [2]. Consequently, the same maximum air temperature may impose

different levels of physiological strain, particularly under humid, windless, or intensely sunny conditions [2]. The World Health Organization recommends that heat-related risks and warning thresholds be assessed in relation to local climate, population vulnerability, and observed health outcomes [3].

The frequency and intensity of hot extremes, including heatwaves, have increased globally since the 1950s, and human influence is assessed as the principal driver of the observed increase over most land regions [4]. The response is nonlinear for threshold-based events: a hot extreme that occurred approximately once per decade in the pre-industrial climate is assessed to occur about 2.8 times per decade at 1 °C of global warming and about 5.6 times per decade at 2 °C [4]. Observational analyses likewise show widespread increases in heatwave frequency, maximum duration, and cumulative seasonal heat, although trends in mean event intensity are less spatially uniform and depend on the metric and analysis period [5]. Consequently, heatwave risk cannot be represented adequately by a change in seasonal mean temperature alone. Event duration, daytime maxima, nocturnal minima, humidity, radiation, wind, antecedent surface conditions, and the timing of exposure all influence the resulting environmental and physiological burden.

Comparison among studies is complicated by the absence of a single universal heatwave definition. Definitions differ in the temperature variable used (daily maximum, minimum, mean, or an apparent-temperature measure), the threshold type (fixed absolute value, local percentile, or health-based threshold), the minimum duration, the reference period, and whether short interruptions are allowed [6]. Absolute thresholds, such as a daily maximum temperature of 30 °C, are readily interpreted and useful for national warning systems, but the same value may represent very different climatological rarity in different regions. Percentile-based definitions facilitate comparison across climatic zones, yet their results remain sensitive to the chosen baseline and may become less representative as the climate shifts. Health-based thresholds are directly relevant to a specified population but are not necessarily transferable between locations or periods. These choices affect the estimated number, duration, severity, and trend of events and may also influence the apparent contrast between coastal and inland sites. A rigorous analysis should therefore state each threshold and temporal rule explicitly and distinguish a heatwave, understood as a persistent meteorological event, from an isolated hot day and from a period of elevated human thermal stress.

Heatwaves also occur within a multivariate and temporally connected hazard environment. Compound events arise when two or more drivers or hazards coincide, occur in sequence, or interact in ways that amplify impacts beyond those expected from either component considered separately [7]. Relevant combinations include high air temperature with elevated atmospheric moisture, hot days followed by warm nights, and heat occurring together with drought, weak ventilation, or high radiant load. Concurrent heat and drought have already become more frequent at the global scale, while dependence-based analyses identify parts of Europe as important hotspots for several compound-hazard combinations [4,8]. Localized observations further indicate that the frequency of extreme humid-heat conditions increased substantially during 1979–2017 and that coarse reanalysis fields may smooth the most severe local values [9]. However, using multivariable thermal indices does not in itself constitute a compound-event analysis, which requires explicit assessment of the joint or sequential occurrence of defined stressors [7]. In this study, complementary thermal-stress indicators describe daytime heat, humidity-related discomfort, and limited nocturnal cooling, bringing these distinct dimensions of thermal exposure into a common climatic assessment. Although some of these indicators are derived from more than one meteorological variable, they are treated as multivariable thermal indices rather than as compound events. The term compound events is reserved here for the concurrent or

sequential occurrence of heat-related hazards, particularly high air temperatures combined with elevated atmospheric humidity and hot days followed by tropical nights. Investigating such compound heat events is becoming increasingly important in coastal regions, where maritime influences may increase atmospheric humidity and limit nocturnal cooling.

The growing relevance of these interconnected dimensions of thermal exposure is further underscored by their implications for human health. The health significance of extreme heat is not confined to tropical or arid climates. A multicountry attribution analysis covering 732 locations estimated that 37% of warm-season heat-related deaths during 1991–2018 were attributable to anthropogenic warming, although the proportion varied geographically [10]. Temperature–mortality relationships vary with the prevailing climate and population adaptation: minimum-mortality temperature ranges are generally lower in cooler regions than in warmer European regions [11]. In the Helsinki region, heat-related mortality remained evident, particularly among older people, while declining sensitivity over successive decades suggested partial adaptation [12]. In Vilnius, an analysis of 2009–2015 data identified increased daily summer mortality at a daily maximum air temperature of 30 °C, corresponding to the 96th percentile of the summer Tmax series, and estimated approximately seven heat-related deaths annually. Future mortality projections depended strongly on the assumed degree of acclimatization [13]. These findings support the population-health relevance of the Tmax ≥ 30 °C threshold examined in the present study, which also underpins Lithuania's official criteria for hazardous heat lasting 1–2 consecutive days and a heatwave lasting at least three consecutive days [14,15]. Together, this evidence highlights the importance of interpreting heat exposure in relation to regional climate, event duration, and population adaptation.

Because air temperature alone does not represent the human heat balance, numerous thermal indices have been developed for different purposes. The Heat Index is a Steadman-derived apparent temperature based principally on air temperature and relative humidity. It does not directly resolve solar radiation or variable wind exposure [16,17]. The broader term Apparent Temperature covers related formulations, some of which additionally include vapour pressure, wind, and radiation, making it essential to report the exact equation used [18]. Humidex combines air temperature with vapour pressure derived from dew-point temperature and is transparent and readily calculated from routine observations, but it omits radiation, wind, activity, and clothing [19]. Such limitations underscore the importance of respecting the applicability limits of heat-stress indices [20] and motivate the use of human heat-balance models that account for the combined effects of air temperature, humidity, wind, and radiation [21].

The Universal Thermal Climate Index (UTCI) provides a more comprehensive, standardized representation of outdoor thermal stress. It uses air temperature, atmospheric moisture, wind speed, and mean radiant temperature within a dynamic multi-node model of human thermoregulation and an adaptive clothing model [22,23]. UTCI is expressed as the equivalent air temperature that would produce the same modeled physiological response under reference conditions, and its standardized stress categories permit comparison across seasons and climatic regions [2,24]. These properties make UTCI an appropriate primary metric for comparing maritime Klaipėda with more continental Vilnius, where radiation, ventilation, humidity, and air temperature may combine differently. Humidex is retained as a complementary index because it offers a simple and interpretable measure of humid heat. The two indices should not be treated as mutual validation: they represent different constructs and share some meteorological inputs. Their joint use instead distinguishes a comprehensive modeled outdoor heat-balance assessment from a humidity-focused metric. Neither index is, by itself, a prediction of individual exposure, morbidity, or mortality.

ERA5 provides a globally complete, physically consistent reconstruction of past atmospheric conditions by combining observations with the ECMWF forecasting system [25]. The ERA5-HEAT product, distributed through the Copernicus Climate Change Service, provides hourly gridded UTCI and mean radiant temperature derived from ERA5 meteorological and radiation variables on a regular 0.25° × 0.25° grid [26,27]. Its principal advantages are homogeneous temporal coverage, standardized computation, and the capacity to place individual locations within a wider regional atmospheric context. These strengths are important where stations do not observe all variables needed for a radiation-sensitive heat-budget index. ERA5-HEAT is derived from ERA5 and characterizes grid-cell-scale thermal conditions rather than point measurements. Coastal cells may combine strong land–sea gradients, while urban form, shoreline geometry, sea-breeze fronts, local cloud, surface properties, and station exposure occur below or near the resolved scale. Consequently, neither the ERA5-HEAT UTCI series nor the ERA5 2 m air-temperature series can be assumed to reproduce every short-lived local maximum or station exceedance of an operational threshold. Previous work at Klaipėda and Nida found substantially fewer ERA5 days than meteorological station days with maximum air temperature ≥ 30 °C, while also showing useful agreement between the two datasets in broader warm-season variability [28]. In situ observations are therefore needed to identify point-scale threshold events and to quantify, rather than presume, station–grid disagreement.

Over Europe, the thermodynamic effect of a warmer background climate interacts with atmospheric dynamics that govern the onset, persistence, and spatial footprint of individual heatwaves. Rousi et al. (2022) found that the number of heatwave days and cumulative heatwave intensity during July–August increased substantially faster in Europe than across the remaining northern mid-latitudes over 1979–2020 [29]. Persistent atmospheric blocking can favour heatwave development and persistence [30], with circulation patterns also linking concurrent events across European regions [31]. Comparing the 2003, 2010, and 2018 European heatwaves, Liu et al. (2020) identified persistent high-pressure systems and atmospheric blocking as common features associated with their development [32].

In the Baltic Sea region, warming and longer warm spells have also been observed, although the contribution of long-term changes in large-scale circulation remains less certain than the thermodynamic warming signal [33]. Lithuania occupies an informative transition between the southeastern Baltic coast and the more continental interior. Analysis of 18 Lithuanian stations for 1961–2010 found increasing recurrence of extremely hot days and nights and showed that persistent anticyclonic circulation types were prominent during these events [34]. More recent coastal research reported increasing heatwave occurrence and tropical nights at Lithuanian seaside stations during 1993–2022 [35]. The maritime influence is potentially dual: the Baltic Sea can suppress daytime maxima through thermal inertia and onshore flow, yet a warm marine surface and humid air can limit nocturnal cooling later in summer. Earlier station evidence likewise showed lower daytime high-temperature percentiles at Klaipėda than in inland Lithuania but relatively elevated late-season nighttime extremes on the coast [34]. A Klaipėda and Vilnius comparison therefore tests more than a simple coast-to-inland temperature gradient; it allows assessment of how maritime moderation, humidity, nighttime heat retention, and synoptic circulation jointly shape heat exposure within the same mid-latitude national setting. Recent scenario-based work in Vilnius combines Humidex with population exposure and age-related vulnerability in the CLIMADA framework [36]. The present study complements that risk-oriented approach through a historical coastal–inland comparison of station extremes, thermal indices and national spatial patterns.

Long-term trends describe the direction of change, whereas spectral analysis can reveal whether temperature anomalies also exhibit preferred multi-year timescales. Considering

both perspectives helps distinguish increasing heat occurrence from recurrent features of temperature variability and provides an additional basis for comparing coastal and inland conditions.

Against this background, the aim of this study is to characterize heatwaves and complementary thermal-stress indicators in Lithuania during 1982–2025, with particular emphasis on maritime-influenced Klaipėda and its contrast with more continental Vilnius within the broader national pattern of temperature extremes. The objectives are to: (i) evaluate agreement between ERA5 air-temperature estimates and meteorological station observations, including the representation of local temperature extremes and threshold exceedances; (ii) assess seasonal and interannual variations in maximum air temperature (Tmax) and long-term changes in the frequency of days with Tmax ≥ 25 °C and ≥30 °C; (iii) investigate whether temperature variability exhibits recurrent multi-year features beyond the long-term warming trend by analysing the spectral structure of monthly Tmax anomalies at Klaipėda and Vilnius after removing the seasonal cycle and linear trend; (iv) characterize the frequency, intensity, seasonality, and temporal changes in daytime thermal stress using ERA5-HEAT UTCI and Humidex indexes, and assess the long-term trends of tropical nights as an indicator of limited nocturnal cooling; and (v) assess spatial patterns across Lithuania using local warm-season 90th-percentile Tmax values, fixed-threshold hot-day and heatwave frequencies, and changes in the magnitude of Tmax exceedances above 30 °C.

By integrating thermal indices, meteorological observations, Copernicus data, spectral analysis, and spatial assessments, the study seeks to provide a basis for understanding coastal–inland differences in heat exposure and informing regional heat-risk assessment. The combined approach examines both long-term changes and recurrent features of temperature variability and employs a set of complementary thermal-stress indicators that jointly capture daytime heat, humidity-related discomfort, and limited nocturnal cooling as complementary dimensions of thermal exposure. Together, this framework links Copernicus-based information with national heatwave criteria to support an integrated assessment of heat stress across Lithuania.

2. Materials and Methods

The study analyses heatwaves and complementary indicators of daytime thermal stress and nighttime heat in the eastern part of the Baltic Sea region in the territory of Lithuania (Figure 1). The study area is dominated by lowlands and plains, and the highlands do not exceed 400 m in height. Lithuania's western coastal region features a transitional maritime climate characterized by milder winters, cooler summers, and higher annual precipitation compared to the continental interior.

The analysis covers the warm season (May–September) during 1982–2025 and contrasts Klaipėda, a Baltic coastal city, with Vilnius, a more continental inland city. Quality-controlled in situ air-temperature observations were obtained from the Lithuanian Hydrometeorological Service (LHMS) for Klaipėda (WMO No. 26509) and Vilnius (WMO No. 26730). These meteorological stations belong to the national meteorological monitoring network and follow WMO observation practices. Changes in instrumentation are validated by LHMS, and the observational records are adjusted where necessary to maintain temporal homogeneity. Neither station was relocated during 1982–2025, and observation methods remained consistent throughout this period. Station daily maximum (Tmax) and minimum (Tmin) air temperatures were used as the local observational reference for fixed-threshold hot days and tropical nights. Gridded fields were obtained from the Copernicus Climate Change Service: ERA5 2 m air and dew-point temperatures were used for air-temperature and Humidex analyses. For UTCI analyses, precomputed daily maxima derived from hourly ERA5-HEAT UTCI were used [25–27]. ERA5 is a model-observation reanalysis, not

a satellite temperature product, and its grid-cell estimates were interpreted as areal rather than point values.

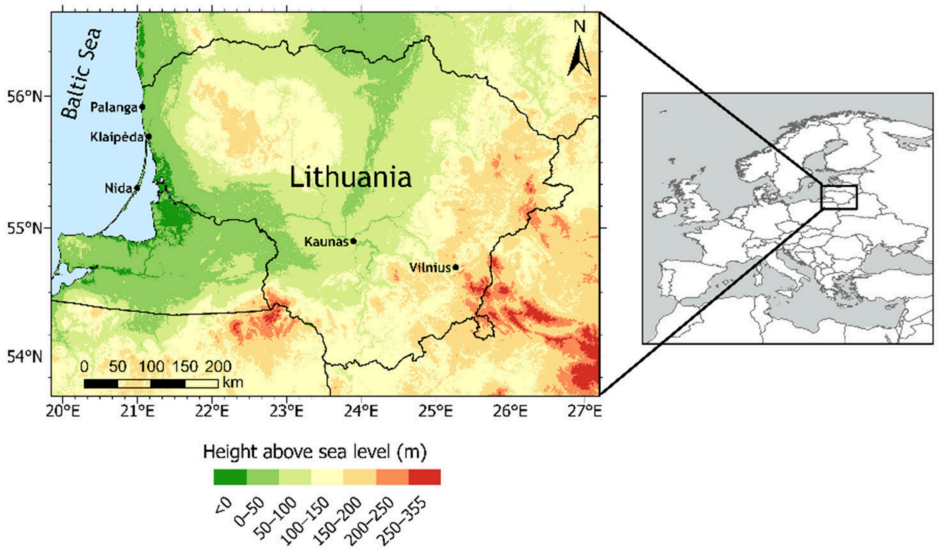

Figure 1. Research area. Meteorological stations performing in situ measurements: Klaipeda (WMO No. 26509) and Vilnius (WMO No. 26730). Locations of Copernicus ERA5 post-processed daily and monthly air temperature (Tmax and Tmin) data (blue squares).

The indices were selected to distinguish how meteorological variables contribute to thermal conditions in this temperate coastal–inland setting. UTCI integrates air temperature, humidity, wind, and radiation within a standardized thermophysiological framework, whereas Humidex describes the temperature–moisture contribution to discomfort. Used alongside Tmax thresholds and tropical nights, they provide complementary information whose relevance can be interpreted in relation to local climate [2,19,22–24,28,35,36].

UTCI was used as the primary multivariable outdoor heat-stress indicator. Daily maximum UTCI values were classified as (i) below the heat-stress threshold (<26 °C), (ii) moderate heat stress (26 to <32 °C), (iii) strong heat stress (32 to <38 °C), (iv) very strong heat stress (38 to <46 °C), and (v) extreme heat stress (≥46 °C) [2,22–24]. Classification was applied before rounding. A UTCI heat-stress day was defined as a day with a daily maximum UTCI ≥ 26 °C. These categories quantify modeled thermo-physiological stress and were not treated as a meteorological heatwave definition or a clinical-risk threshold.

Humidex (H) was calculated from hourly ERA5 2 m air temperature (T) and 2 m dew-point temperature (Td), using the formulation of Masterton and Richardson [19] (Masterton and Richardson, 1979):

$$H = T + 0.5555 * (e - 10)$$

$$e = 6.11 * exp[5417.7530 * (1/273.16 - 1/(273.15 + Td))]$$

Here, air temperature (T) and dew-point temperature (Td) are expressed in °C, and water vapour pressure (e) is expressed in hPa. For each day, H was evaluated at the hour of the daily maximum air temperature (Tmax), using the concurrent dew-point temperature. Humidex values are reported in °C, following the convention used in the Copernicus Climate Data Store documentation [37] (Iles et al., 2021). Categories follow the classification presented by the European Centre for Medium-Range Weather Forecasts (ECMWF): little discomfort ($20 \leq H < 30$), some discomfort ($30 \leq H < 40$), great discomfort, avoid exertion ($40 \leq H < 46$), and dangerous, possible heat stroke ($H \geq 46$) [38] (ECMWF,

2024). Throughout this study, the categories corresponding to these levels are termed: comfortable, moderate discomfort, high discomfort, and danger.

Daily temperature and thermal-index comparisons at both locations covered May–September during 1982–2025. Records were aligned by calendar date and paired using available values for the variables compared. Thresholds were then applied to identify hot days and thermal-stress categories within this period. UTCI retained its daily maximum definition, while Humidex was evaluated both at the hour of Tmax and as the daily maximum calculated from hourly values. Using daily maxima provides a consistent basis for comparing the indices, although their maxima may occur at different hours. The comparison therefore describes daily thermal conditions rather than conditions occurring simultaneously.

An extremely hot day was defined as a day with Tmax ≥ 30 °C, and a tropical night as a night with Tmin ≥ 20 °C. Consecutive tropical nights were grouped into uninterrupted episodes. Trends in the annual number of tropical nights and the annual maximum episode duration were analysed over the study period. Station observations and ERA5 daily maximum air temperatures were compared over matching periods to evaluate temporal agreement and event detection.

Extremely hot days and heatwaves were also identified across the whole territory of Lithuania to assess their recurrence and spatial distribution. To do that, daily maximum air temperature (Tmax) data from the European Centre for Medium-Range Weather Forecasts (ECMWF) ERA5 reanalysis were used [39]. The spatial resolution of the grid cells was 0.25° × 0.25°. Only data from grid cells that included at least a small part of Lithuania's territory were used in the analysis. The coastal values describe the retained ERA5 cells, which may include a substantial marine contribution.

According to the official methodology used in Lithuania, a hot day is defined as a day on which Tmax ≥ 30 °C [14]. When the 30 °C threshold is reached or exceeded for at least three consecutive days, a heatwave is identified, which is classified as a hazardous meteorological event (otherwise named severe) [15] that can cause severe stress and even threaten human life. The frequency of hot days was determined for the standard climate normal (1991–2020).

Changes in the number of such days were also determined by comparing the number of hot days during the first (1982–2001) and last (2006–2025) 20-year periods of the study. The 20-year periods, which are also used in IPCC reports [40] (Chen, 2021), were selected to compare hot-day recurrence between the beginning and end of the record during a period of climatic warming. In addition, the aim was to ensure that the two periods did not overlap. The equal-length windows leave 2002–2005 outside this contrast, while trend analyses use all 44 years. Differences were screened locally using the Mann–Whitney–Wilcoxon test with unadjusted $p < 0.05$. Because many spatially correlated tests are performed simultaneously, the local p-values were adjusted using the Benjamini–Hochberg false discovery rate (FDR) procedure [41] (Benjamini and Hochberg, 1995), with the FDR level set to 0.05. The results were mapped to show the spatial distribution of changes. In addition, the number of heatwaves over the entire study period (1982–2025) was calculated for each grid cell within the study area. Finally, the mean deviations of Tmax from the 30 °C threshold during the hot days were assessed, and changes in this indicator were determined by comparing the periods 1982–2001 and 2006–2025. The same Mann–Whitney–Wilcoxon test and Benjamini–Hochberg FDR adjustment were applied to changes in mean Tmax exceedance above 30 °C on hot days.

As the study covers only Lithuania, the country's official indicators were used to identify hot days and heatwaves. Nevertheless, when assessing heatwaves at regional or global scales, a percentile-based approach is often applied. There is no universal consensus

on which percentile threshold to use to identify heatwaves, but under this approach, a heatwave is defined as exceeding the selected percentile threshold for at least several consecutive days. One commonly used threshold is the 90th percentile. It has been widely applied in studies of heatwaves across different regions of Europe [29,42,43], as well as in the Baltic States and other European regions [44–48]. Here, the 90th percentile was used to describe spatial temperature contrasts, while heatwaves were identified using the national criterion of Tmax ≥30 °C for at least three consecutive days.

Annual day and night counts were regressed on year using ordinary least squares (OLS) to estimate the long-term rate of change. For statistical inference, Newey–West covariance estimates [49] (Newey and West, 1987) were calculated using Bartlett weights and a maximum lag of three years. This lag is consistent with the sample-size expression 4(n/100)^(2/9) applied by Wahl and Plant [50] (2015), rounded down to an integer for $n = 44$ annual observations. A finite-sample correction of 44/42 and a Student's t distribution with 42 degrees of freedom were used for confidence intervals and two-sided tests. The Ljung–Box diagnostic [51] (Ljung and Box, 1978) examined residual autocorrelation jointly over lags 1–4 to assess short-range temporal dependence.

Climate time series may exhibit enhanced spectral power at particular timescales. However, such spectral peaks do not necessarily indicate regular or deterministic cycles. Therefore, this study examined whether monthly mean Tmax anomalies exhibit preferred multi-year variability timescales after removal of the seasonal cycle and linear trend. For this purpose, the Welch power spectral density (PSD) estimator, based on averaging overlapping modified periodograms, was applied [52]. In climatological research, this method, or equivalent spectral averaging approaches based on overlapping segments, has been used to investigate variability in meteorological time series across timescales ranging from days to decades [53], monthly tropospheric temperature anomalies [54], and multi-year variability in station air-temperature records [55].

The spectral analysis used station time series from Klaipėda and Vilnius comprising all 528 months from January 1982 to December 2025. Monthly mean Tmax values were first calculated from daily maximum temperatures. The seasonal cycle was removed by subtracting from each monthly value the corresponding calendar-month climatological mean calculated for 1982–2025. A linear trend was subsequently removed from each anomaly series. Consequently, the spectral analysis characterizes residual Tmax variability around the seasonal cycle and linear trend rather than the long-term warming signal itself.

For each station, the detrended 44-year monthly time series was divided into 20-year (240-month) segments with 50% overlap (120 months). A Hamming window was applied to each segment, and a modified Fourier periodogram was calculated using a sampling frequency of 12 observations per year and 4096 FFT points. The resulting spectral estimates were averaged to obtain the Welch power spectral density (PSD). The Welch PSD approach was used to identify the multi-year timescales of enhanced variability in the detrended monthly Tmax anomalies for Klaipėda and Vilnius during 1982–2025 and to compare the spectral estimates with pointwise Monte Carlo-derived AR(1) red-noise thresholds.

To establish station-specific red-noise references, a first-order autoregressive [AR(1)] model was fitted separately to each station's detrended monthly anomaly series. The fitted model provides a reference for evaluating spectral peaks while accounting for the correlation between successive monthly anomalies. For each station, 1000 Monte Carlo realizations of the fitted AR(1) process were generated and analysed using the same Welch procedure. At each frequency, the 95th percentile of the simulated PSD values was calculated and used as the pointwise 95% AR(1) red-noise significance threshold. A peak exceeding this threshold has greater spectral power than 95% of the simulated values at the same frequency. Red-noise backgrounds are widely used as a reference for assessing the significance of

spectral features in climatic time series [56–58]. The displayed periods span 2–15 years. These periods describe the timescales of the temperature fluctuations examined, rather than the dates covered by the observational record. These thresholds represent pointwise rather than global significance levels, and no correction for multiple comparisons across frequencies was applied. Consequently, spectral peaks exceeding these thresholds were interpreted as exploratory indications of enhanced variability at individual timescales rather than statistically confirmed periodicities. In this study, spectral analysis was used to compare the dominant timescales of temperature variability between Klaipėda and Vilnius, complementing the trend analysis by examining fluctuations in the detrended series. These findings provide a basis for further comparative spectral studies.

3. Results

3.1. Comparison of In Situ and ERA5 2 m Air-Temperature Data

In situ observations and Copernicus ERA5 2 m air-temperature estimates were compared to assess how well ERA5 represents temperature variability and high air temperature conditions at coastal Klaipėda and inland Vilnius. This assessment provides the basis for using ERA5 in the regional analysis and establishes its agreement with local observations. The comparison covers the warm season, May–September, when the highest daily maximum air temperatures generally occur.

The year 2024 was selected for the daily Tmax and Tmin comparison because several heatwaves were recorded in Lithuania during that year. This allowed ERA5 performance during station-observed high-temperature episodes to be examined (Figure 2a–d). The 2024 series therefore illustrates the correspondence between daily temperature changes in the two datasets during a season with observed heatwaves, whereas the annual counts in Figure 2e,f place the threshold exceedances within the full 1982–2025 record.

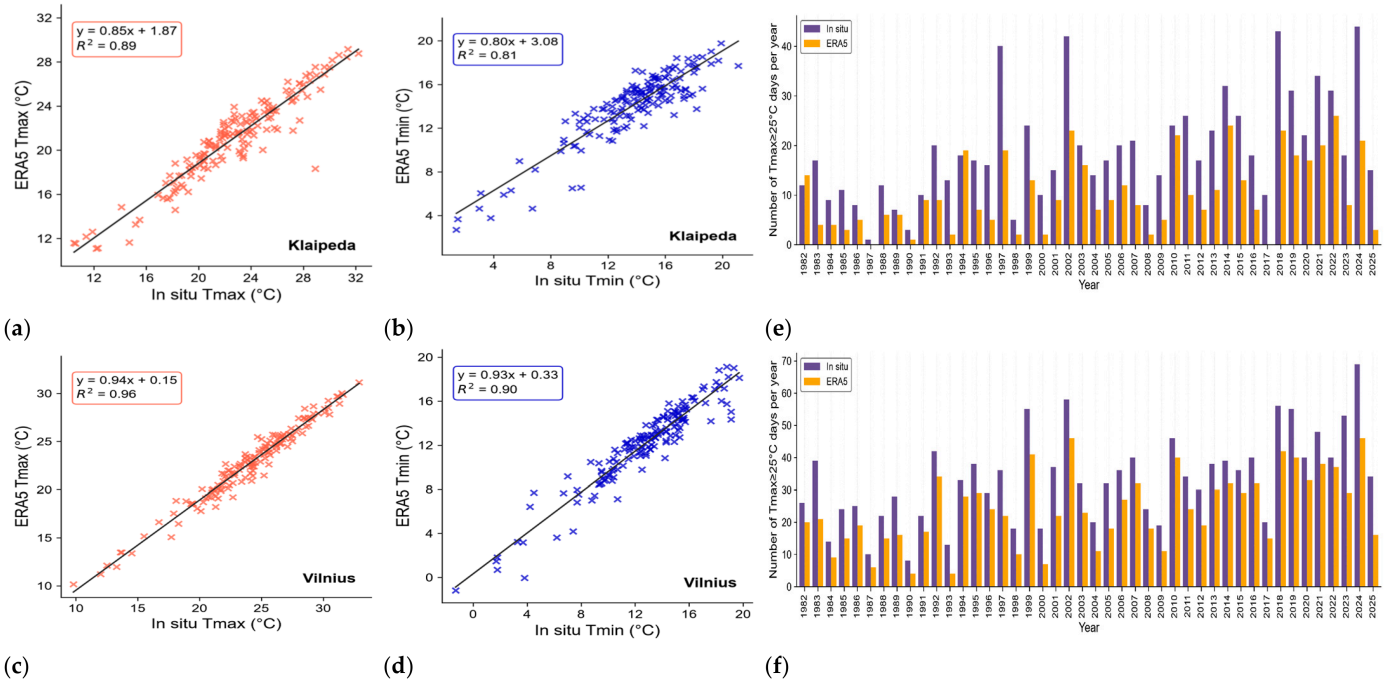

Figure 2. Comparison between in situ observed and Copernicus ERA5 daily temperatures during the warm season (May–September) of 2024 at Klaipėda and Vilnius: (**a**) Tmax at Klaipėda; (**b**) Tmin at Klaipėda; (**c**) Tmax at Vilnius; (**d**) Tmin at Vilnius. Comparison of the annual number of Tmax ≥ 25 °C days per year between in situ observations and Copernicus ERA5 data over 1982–2025: (**e**) Klaipėda, (**f**) Vilnius.

Station observations and ERA5 air-temperature estimates showed a close relationship, with stronger agreement at Vilnius than at Klaipėda (Figure 2). This supports the use of ERA5 for examining broad temperature variability. The larger discrepancy at Klaipėda is consistent with the difference between point measurements and the area represented by a 0.25° × 0.25° reanalysis grid cell, particularly near the land–sea boundary (Figure 1). Klaipėda showed a bias of −1.12 °C, MAE of 1.51 °C, RMSE of 1.94 °C and r = 0.94. The corresponding Vilnius values were −1.02 °C, 1.12 °C, 1.44 °C and r = 0.98. These correlations show that ERA5 closely followed daily temperature variability at both stations. The negative biases indicate lower temperatures in ERA5 on average, while the smaller mean absolute error (MAE) and RMSE at Vilnius demonstrate closer agreement with the inland observations.

Agreement during high-temperature conditions was assessed separately because the full-season statistics include both cooler and warmer days. For the evaluated Klaipėda station–grid pairing, ERA5 reproduced the broad warm-season temperature variability but underestimated the annual number of station-observed days with Tmax ≥ 25 °C in many years (Figure 2e). The corresponding comparison for Vilnius is shown in Figure 2f.

The root-mean-square error (RMSE) quantifies the typical magnitude of the day-to-day discrepancy between the two datasets, combining both the systematic bias and the dispersion around it (Figure 3). For the selected sample in Figure 3, bias is the mean difference between ERA5 and in situ Tmax (ERA5−observations), averaged over matched days with station Tmax ≥ 25 °C. Unlike the bias, positive and negative errors do not cancel out in the RMSE calculation, so RMSE is always greater than or equal to the absolute value of the bias. For the Tmax ≥ 25 °C comparisons in Figure 3, the plotted bias and RMSE are −2.48 and 2.94 °C at Klaipėda, compared with −1.21 and 1.59 °C at Vilnius. The negative biases show that ERA5 underestimated Tmax on these observed high-temperature days at both stations. The larger absolute bias and RMSE at Klaipėda indicate a greater discrepancy at the coast. These estimates apply specifically to the station-selected Tmax ≥ 25 °C sample and are distinct from the statistics calculated over all matched warm-season dates.

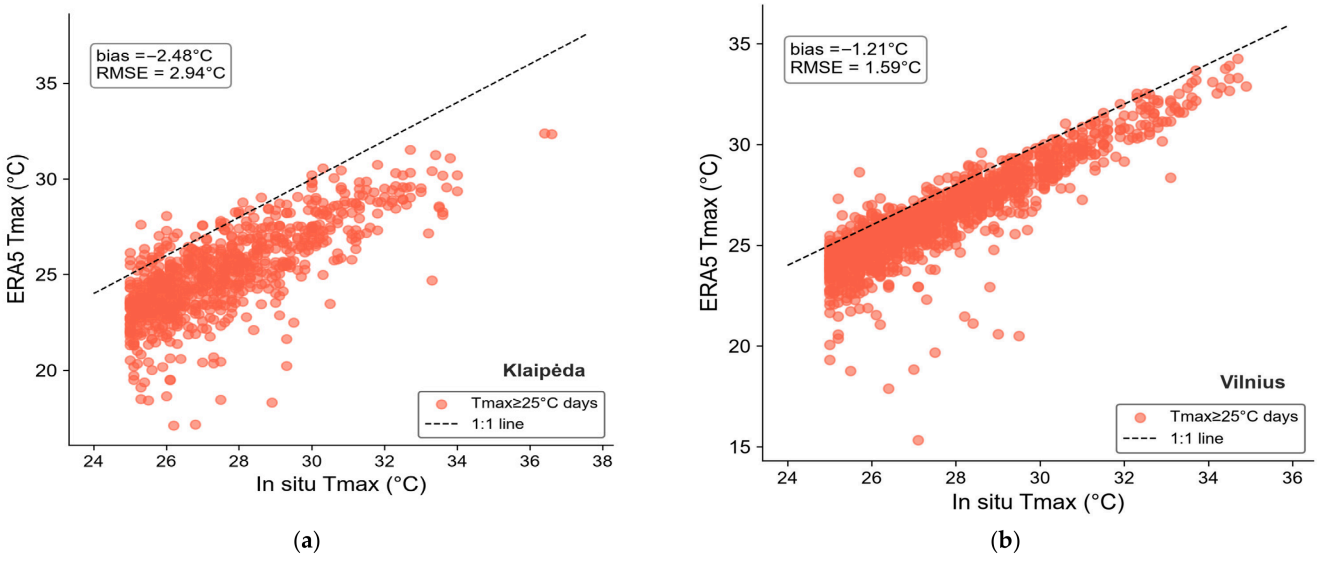

Figure 3. Comparison between in situ and ERA5 daily maximum air temperatures on days with station Tmax ≥ 25 °C at (**a**) Klaipėda and (**b**) Vilnius during 1982–2025. Mean bias (ERA5 minus observations) and root-mean-square error (RMSE) are shown in each panel.

The effect of these temperature discrepancies on the identification of threshold exceedances was quantified at 25 °C and 30 °C. At 25 °C, ERA5 detected 50.4% of observed exceedances in Klaipėda and 71.4% in Vilnius, with precision of 92.5% and 99.1%, re-

spectively. Here, detection describes the proportion of station-observed exceedances also identified by ERA5, whereas precision describes the proportion of ERA5 exceedances confirmed by station observations. Missed-event rates were 49.6% and 28.6%, and false-positive rates were 0.58% and 0.17%. At 30 °C, sensitivity was 12.6% and 49.5%, respectively, with missed-event rates of 87.4% and 50.5%; no false-positive exceedances occurred in either matched sample. Thus, ERA5 exceedances were usually confirmed by observations, but ERA5 missed a substantial proportion of observed high-temperature days. Detection was lower at the higher threshold and consistently lower at Klaipėda than at Vilnius.

The heatwave comparison assessed whether ERA5 also captured the persistence of high temperatures, using the same national criterion in both datasets: at least three consecutive days with Tmax ≥ 30 °C. Station observations identified 12 heatwaves comprising 42 days in Klaipėda and 23 heatwaves comprising 96 days in Vilnius. The longest lasted 5 and 8 days, respectively. On the corresponding available dates, ERA5 identified no heatwaves in Klaipėda and 13 in Vilnius, comprising 48 days with a maximum duration of 5 days. All 13 Vilnius ERA5 events overlapped with observed events, giving detection of 13 of 23 observed events (56.5%) and no unmatched ERA5 events. Although all ERA5 heatwaves at Vilnius corresponded to observed events, ERA5 recorded fewer events, fewer heatwave days, and a shorter maximum duration. The discrepancy was greater at Klaipėda, where ERA5 identified no heatwaves meeting the three-day criterion.

Together, the full-season, threshold and heatwave comparisons show which aspects of the observed temperature regime are represented by ERA5. The close correspondence in daily variability supports its use for examining the regional thermal setting, while the negative biases and missed exceedances demonstrate the importance of station observations for identifying local high-temperature days and determining whether their intensity and persistence meet the national criteria for a hazardous heatwave event.

The subsequent UTCI and Humidex analyses extend this comparison from air temperature to thermal-stress indicators that incorporate additional meteorological conditions. ERA5 provides a consistent meteorological dataset for examining their spatial patterns, long-term changes and exceedance frequencies over the study period. The station comparison establishes the context for interpreting these results: the identified temperature biases are relevant to absolute index values and threshold exceedances, particularly at the coast, although they do not directly quantify the errors in UTCI or Humidex. Accordingly, the analysis focuses on long-term changes and coastal–inland contrasts in the ERA5-derived indicators, with station observations providing the local evidence for high-temperature extremes.

3.2. Changes and Trends in Maximum Air Temperature (Tmax)

Monthly Tmax patterns for 1982–2025 show pronounced seasonal and interannual variability at both analysed stations (Figure 4). The highest monthly Tmax values occur during the warm season, particularly from June to August. Vilnius generally exhibits higher summer Tmax than Klaipėda, whereas the coastal station shows a more moderated annual temperature regime, consistent with the maritime influence of the Baltic Sea. The diagrams also indicate that high summer Tmax values have become more frequent in the later part of the record, although substantial year-to-year variability remains.

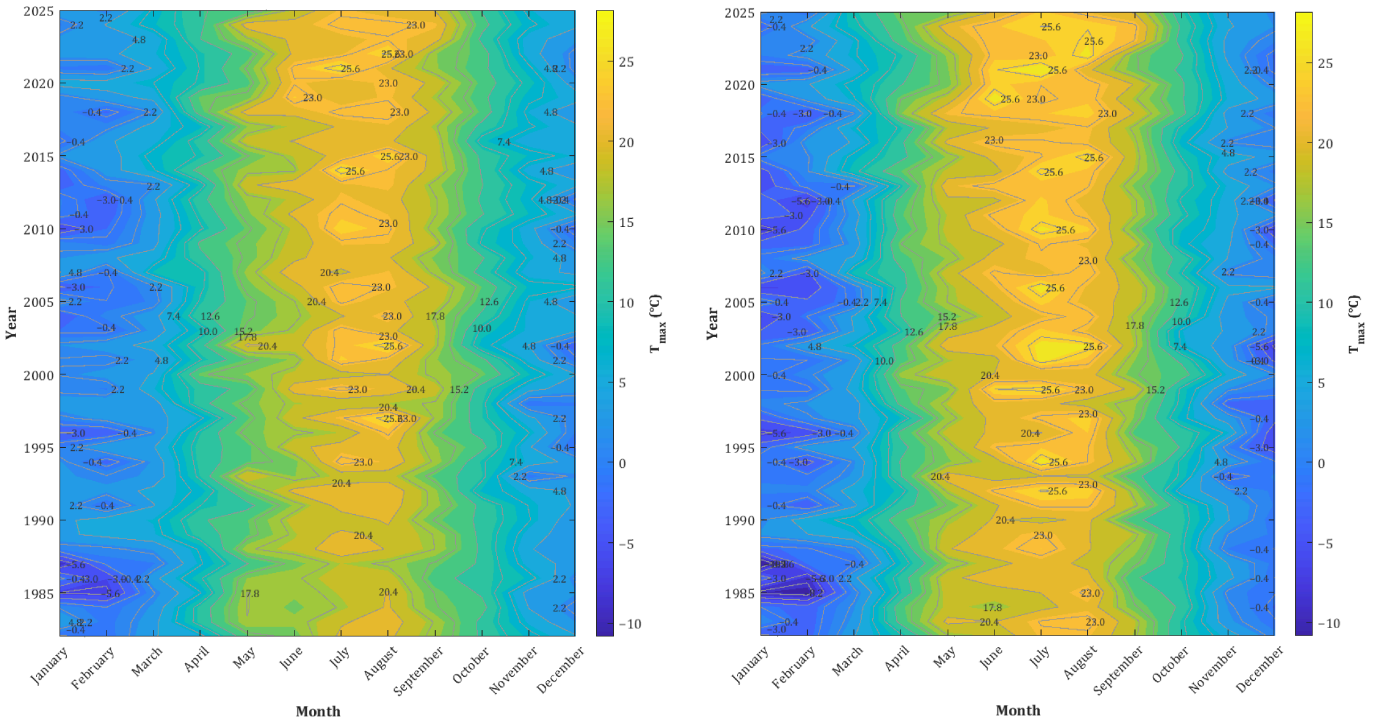

Figure 4. Monthly mean daily maximum air temperature (Tmax) during 1982–2025 based on in situ observations: (**a**) Klaipėda, (**b**) Vilnius.

During 1982–2025, the annual numbers of days reaching both Tmax thresholds increased at Klaipėda and Vilnius, although pronounced year-to-year variability remained (Figure 5). This long-term change is also evident in the annual frequency of hot days. In Klaipėda, the number of days with Tmax ≥ 25 °C increased by approximately 4.58 days per decade, while days with Tmax ≥ 30 °C increased by about 1.55 days per decade. The corresponding trends in Vilnius were stronger, reaching approximately 5.96 and 1.77 days per decade, respectively. Thus, the continental station had a higher frequency of high-Tmax conditions and larger estimated increases at both thresholds than maritime Klaipėda. All OLS (Ordinary Least Squares) slope tests were statistically significant ($p \leq 0.0015$), but the regressions explained only 21.6–31.0% of the annual variance, indicating substantial interannual fluctuations. The highest numbers of Tmax ≥ 25 °C days occurred in 2024 (44 days at Klaipėda and 69 at Vilnius). The series maximum for Tmax ≥ 30 °C was 16 days, recorded at Klaipėda in 2014 and at Vilnius in 2021 and 2022.

To assess whether temporal dependence affected the statistical significance of these trends, the same 1982–2025 annual series were examined using residual autocorrelation diagnostics, including the Ljung–Box test [51] and Newey–West standard errors [49]. This assessment retained the original OLS slopes while accounting for possible serial correlation and unequal residual variance in their uncertainty estimates. Residual lag-1 autocorrelations ranged from −0.225 to 0.089, and Ljung–Box *p*-values through lag 4 ranged from 0.106 to 0.697, providing no statistically significant evidence of residual autocorrelation at the examined lags. All four positive trends remained statistically significant under the Newey–West assessment ($p < 0.001$). The corresponding 95% confidence intervals for the increases in days with Tmax ≥ 25 °C and Tmax ≥ 30 °C were, respectively, 3.01–6.15 and 0.95–2.16 days per decade at Klaipėda, and 3.74–8.17 and 0.84–2.70 days per decade at Vilnius. All intervals remained above zero, supporting an increase at both temperature thresholds and both stations despite the substantial year-to-year variability.

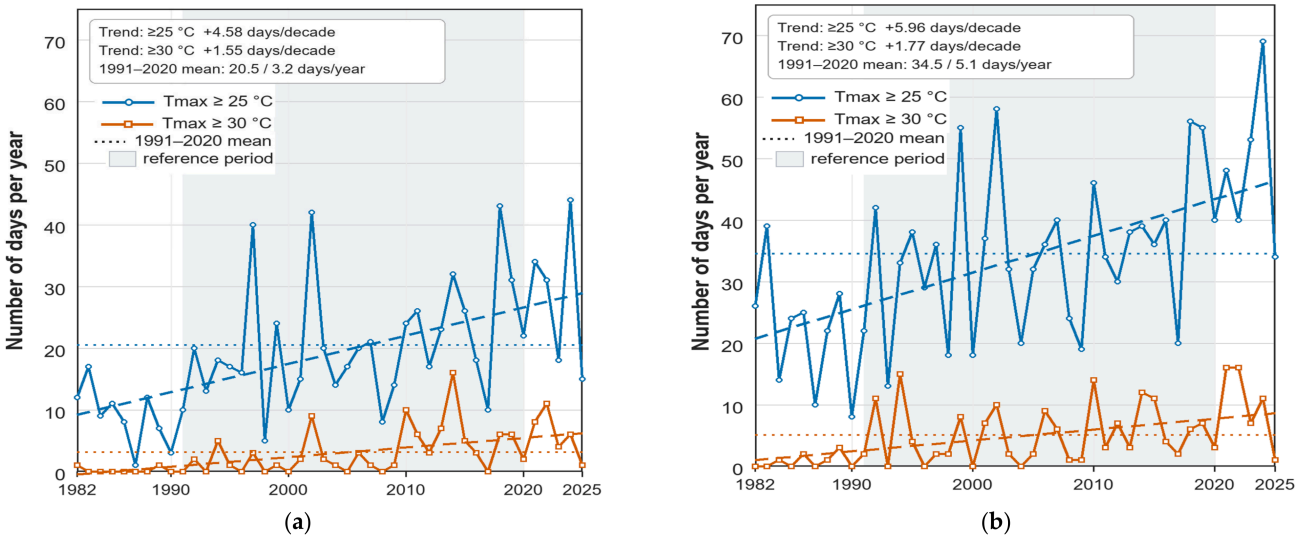

Figure 5. Annual number of days with Tmax ≥ 25 °C and Tmax ≥ 30 °C during 1982–2025 and corresponding linear trends: (**a**) Klaipėda and (**b**) Vilnius. The reference period is the 1991–2020 climatological reference period, used to calculate the climate norm. The gray area only shows the boundaries of this reference period (from 1991 to 2020). The horizontal dotted lines show the 1991–2020 mean annual numbers of days with Tmax ≥ 25 °C (blue) and Tmax ≥ 30 °C (orange), both represented by the black dotted line in the legend.

The heatwave analysis complements the annual day counts by examining consecutive high-temperature days as distinct events. Heatwaves lasting three or more consecutive days with Tmax ≥ 30 °C meet Lithuania's national criterion for a severe meteorological event [15]. Comparing the first (1982–2001) and last (2006–2025) 20-year periods, the number of heatwaves meeting this criterion increased from 1 to 10 in Klaipėda and from 5 to 16 in Vilnius, while the total number of heatwave days increased from 3 to 35 and from 23 to 66 days, respectively. Thus, the later period contained more heatwaves meeting the national severe-event criterion and more days within these events at both stations.

In Vilnius, the 69 days with Tmax ≥ 25 °C recorded in 2024 represented almost twice the 1991–2020 climatological mean of 34.53 days per year (Figure 5). The 1991–2020 climatological means demonstrate a clear coastal–inland contrast. Both the mean annual count and its interannual variability were higher in Vilnius. Klaipėda averaged 20.53 ± 9.57 days per year with Tmax ≥ 25 °C and 3.17 ± 3.71 days per year with Tmax ≥ 30 °C, whereas Vilnius averaged 34.53 ± 12.02 and 5.13 ± 4.42 days per year, respectively (mean ± interannual standard deviation). Thus, during the reference period, Vilnius experienced approximately 14 more Tmax ≥ 25 °C days and two more Tmax ≥ 30 °C days per year than Klaipėda. This descriptive difference is consistent with stronger maritime moderation at the coastal station and a more continental thermal regime inland.

During 2021–2025, Klaipėda averaged 28.4 days per year with Tmax ≥ 25 °C and 6.0 days per year with Tmax ≥ 30 °C, whereas Vilnius averaged 48.8 and 10.2 days per year, respectively. These five-year mean annual counts exceeded the corresponding 1991–2020 climatological means at both stations and both thresholds, complementing the increasing trends identified over the full 1982–2025 record. The frequency of high-temperature days remained higher in Vilnius, preserving the coastal–inland contrast in the recent period. At the same time, individual years deviate strongly from the long-term trend, emphasizing the importance of analysing both climatic trends and multi-year variability. Accordingly, the following section examines whether the residual Tmax variability, after removal of the seasonal cycle and linear trend, contains preferred multi-year timescales.

3.3. Long-Term Spectral Structure of Monthly Tmax Anomalies

The analysed period was characterized by a clear warming tendency and a pronounced increase in maximum air temperatures (Tmax). To examine whether the remaining temperature variability exhibits preferred multi-year timescales, monthly mean Tmax anomaly series derived from in situ observations at the Klaipėda and Vilnius meteorological stations for 1982–2025 were analysed using the Welch power spectral density (PSD) method (Figure 6). Prior to the spectral analysis, the seasonal cycle and linear trend were removed, allowing the analysis to focus on residual Tmax variability rather than the long-term warming signal.

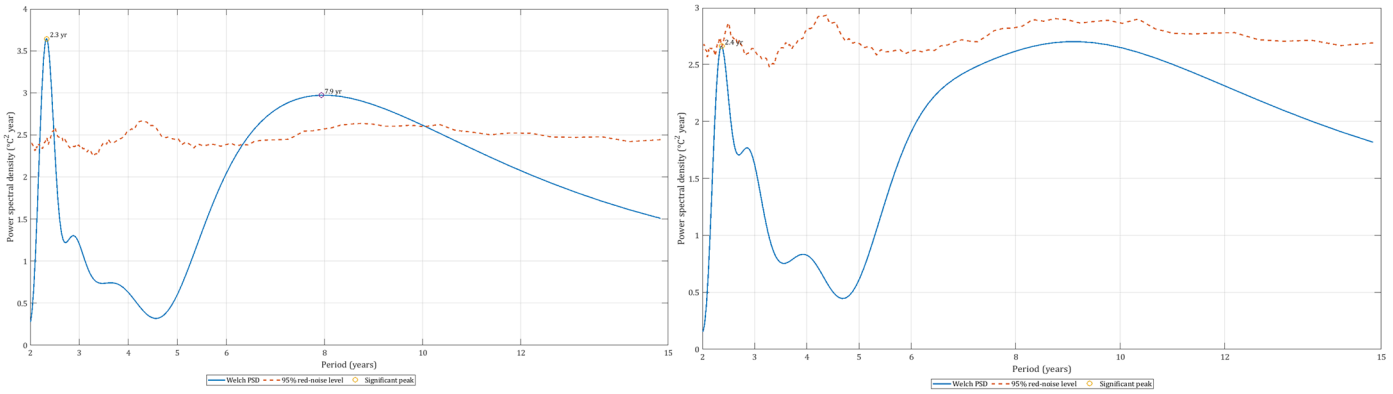

(**a**) (**b**)

Figure 6. Welch power spectral density (PSD) of monthly Tmax anomalies derived from in situ observations at the meteorological stations: (**a**) Klaipėda and (**b**) Vilnius. The x-axis represents the period in years, and the y-axis represents power spectral density (PSD). The blue curve (Welch PSD) shows the spectrum of Tmax anomalies and the spectral power associated with each timescale. The red dashed line is the pointwise 95th percentile from 1000 AR(1) Monte Carlo realizations. Peaks above it identify exploratory spectral enhancements at the corresponding frequencies.

The estimated first-order autoregressive coefficients were AR(1) = 0.254 for Klaipėda and AR(1) = 0.204 for Vilnius. Both values indicate weak positive month-to-month persistence in the monthly Tmax anomalies, with slightly weaker short-term persistence in Vilnius than in Klaipėda. These coefficients characterize the short-term temporal dependence of the time series. But they do not explain the physical mechanisms underlying the observed spectral peaks.

The Klaipėda spectrum revealed two peaks exceeding the pointwise 95% AR(1) red-noise threshold derived from Monte Carlo simulations (Figure 6a; Table 1). The strongest peak occurred at approximately 2.34 years, with spectral power exceeding the corresponding 95% threshold by approximately 48%. This result indicates enhanced Tmax anomaly variability at a timescale of approximately 2–3 years.

A second, weaker spectral peak in Klaipėda occurred at approximately 7.94 years and exceeded the corresponding threshold by approximately 16%. The peak was broader and less pronounced than the 2.34-year peak and is therefore more appropriately interpreted as enhanced variability within a broader 7–9-year timescale rather than as a regular cycle. Moreover, a 20-year Welch segment contains only about 2.5 oscillations of this duration, limiting the precision with which the position of such a low-frequency spectral peak can be determined.

Table 1. Main spectral peaks and their statistical characteristics in monthly Tmax anomalies at Klaipėda and Vilnius meteorological stations. Note: The 95% threshold was derived pointwise from AR(1) red-noise Monte Carlo simulations. Values above the threshold indicate spectral peaks exceeding the pointwise 95% significance level.

Station	Timescale (Years)	PSD	95% AR(1) Threshold	PSD/ Threshold	Interpretation
Klaipėda	2.34	3.6427	2.4692	1.48	Clear exceedance (~48%); enhanced 2–3-year variability
Klaipėda	7.94	2.9723	2.5661	1.16	Moderate exceedance (~16%); broader 7–9-year variability
Vilnius	2.37	2.6605	2.6548	1.002	Marginal exceedance (~0.2%)
Vilnius	9.23	~2.67	~2.94	0.908	Below threshold (~9%); broad low-frequency maximum

In Vilnius, a spectral peak occurred at approximately 2.37 years (Figure 6b, Table 1). However, its PSD exceeded the corresponding pointwise 95% threshold by only approximately 0.2%. Thus, although the peak formally lies slightly above the 95% threshold, the very small exceedance indicates only marginal statistical evidence. Exceedance of this threshold indicates locally enhanced spectral power relative to the AR(1) background, but does not establish global statistical significance across the frequency spectrum. A broader spectral maximum was also observed at approximately 9.23 years, but it remained below the 95% threshold. Its spectral power was approximately 9% lower than the corresponding threshold. Therefore, this feature can only be interpreted as a region of enhanced spectral power and not as a statistically significant periodic component. Accordingly, the identified spectral peaks are interpreted as exploratory evidence of preferred variability timescales rather than confirmed periodic cycles.

In summary, the spectra showed closely corresponding shorter-period maxima at 2.34 years in Klaipėda and 2.37 years in Vilnius, together with broader maxima at 7.94 and 9.23 years, respectively. The longer-period maximum exceeded the pointwise 95% AR(1) threshold only in Klaipėda. Although Klaipėda and Vilnius represent different climatic settings approximately 300 km apart, their shorter-term spectral maxima occur at closely corresponding periods. The Klaipėda peak is more pronounced relative to its pointwise AR(1) reference, whereas the Vilnius peak lies only marginally above that reference. The comparison therefore highlights a similar 2–3-year variability timescale with different local spectral expression. However, an important limitation of the spectral analysis is that the Monte Carlo-derived 95% AR(1) thresholds were evaluated pointwise, without correction for multiple comparisons across the examined frequencies. Therefore, threshold exceedances should not be interpreted as evidence of globally significant periodicities.

Overall, this exploratory spectral analysis complements the linear trend analysis by identifying the multi-year timescales over which residual monthly Tmax variability is concentrated. The closely corresponding shorter-period maxima and broader features provide a basis for examining whether coastal and inland stations share common patterns of temperature variability. Future analyses using longer records and a wider station network could assess the temporal stability and spatial coherence of these features, evaluate their relationships with atmospheric circulation and Baltic Sea conditions, and apply significance tests that account for multiple comparisons. Such work could help clarify how multi-year variability influences temperature trends estimated over different observation periods, supporting a more robust interpretation of long-term temperature change.

3.4. Complementary Thermal-Stress Indicators

The results indicate an increasing frequency of heat-stress conditions in Lithuania. The annual number of days with heat stress (UTCI ≥ 26 °C) showed a positive linear trend at both research locations during 1982–2025 (Figure 7). Fewer heat-stress days were recorded in the location with a maritime climate (Klaipėda) than in the location with a continental climate (Vilnius). During the May–September seasons of 1982–2025, a total of 562 days with moderate or stronger heat stress (UTCI ≥ 26 °C) were recorded in Klaipėda and 1608 in Vilnius. These counts include days with moderate and more severe heat stress. The annual number of such days increased more rapidly in Vilnius. The fitted rates were +0.30 days per year in the ERA5-HEAT grid cell representing Klaipėda ($R^2 = 0.24$) and +0.61 days per year in the cell representing Vilnius ($R^2 = 0.34$). The increases were statistically significant using Newey–West standard errors, which account for potential temporal dependence and unequal variance in the regression errors. The corresponding 95% confidence intervals for the slopes were 0.18–0.43 days per year in Klaipėda and 0.45–0.76 days per year in Vilnius (both $p < 0.001$). Both intervals were entirely above zero, supporting an increase in the annual number of heat-stress days at both locations. Expressed per decade, the fitted trends correspond to approximately 3 additional days with UTCI ≥ 26 °C in Klaipėda and 6 in Vilnius. These long-term increases were accompanied by interannual variability in the number of heat-stress days. These results could be useful for sustainability planning, as the estimated long-term rates of change could inform climate adaptation measures.

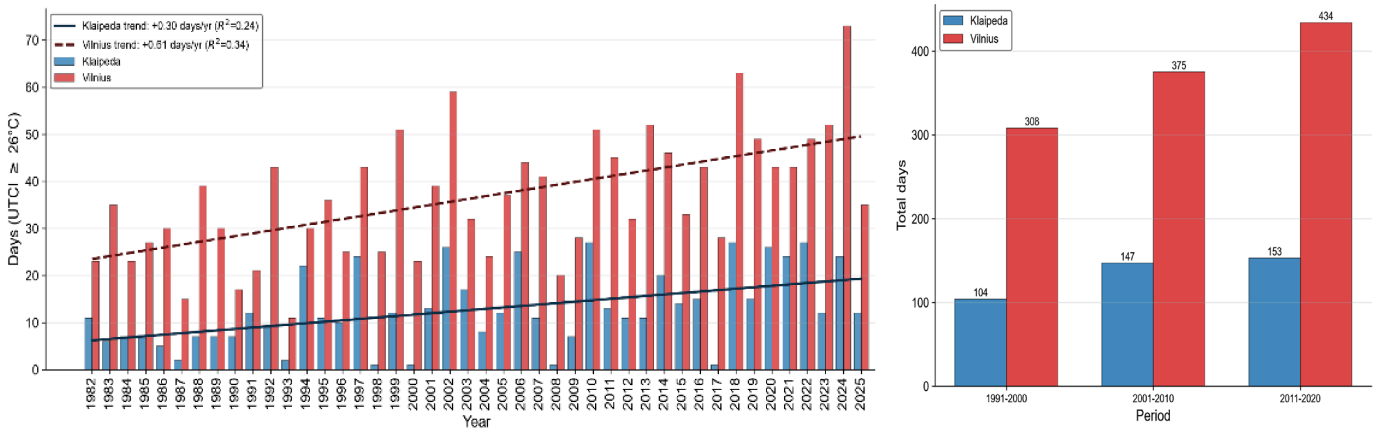

(**a**) (**b**)

Figure 7. ERA5-HEAT UTCI heat-stress days (daily maximum UTCI ≥ 26 °C) in the grid cells representing Klaipėda and Vilnius: (**a**) annual warm-season counts during 1982–2025, with ordinary least-squares fits (Klaipėda: $\beta = +0.30$ days yr^{-1}, $R^2 = 0.24$; Vilnius: $\beta = +0.61$ days yr^{-1}, and $R^2 = 0.34$); (**b**) total heat-stress-day counts for 1991–2000, 2001–2010, and 2011–2020.

The decadal totals of UTCI heat-stress days increased across the three decades, 1991–2000, 2001–2010, and 2011–2020, at both locations (Figure 7b), indicating more frequent exceedance of the UTCI heat-stress threshold in the later decades. UTCI heat-stress days occurred over a broader warm-season window in Vilnius, whereas their distribution in Klaipėda was more concentrated in summer (Figure 8). At both locations, the highest monthly counts generally occurred during June–August.

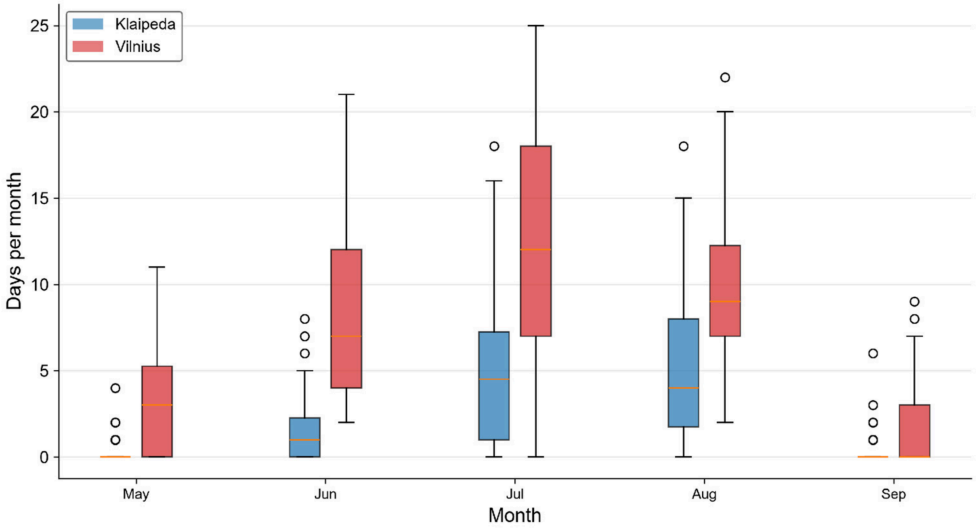

Figure 8. Monthly counts of UTCI heat-stress days (daily maximum UTCI ≥ 26 °C) in the ERA5-HEAT grid cells representing Klaipėda and Vilnius during May–September 1982–2025. Blue and red boxes represent Klaipėda and Vilnius, respectively. Boxes show the interquartile range, horizontal lines indicate medians, whiskers extend to the most extreme observations within 1.5 times the interquartile range, and open circles denote outliers.

Figure 9 shows clear differences in the seasonal distribution and intensity of heat stress between the two cities. In Klaipėda (Figure 9a), heat-stress days were relatively sparse and concentrated mainly between late June and late August, whereas in Vilnius (Figure 9b) they were considerably more numerous and occurred over a broader period extending from May to September. Vilnius also experienced higher daily maximum UTCI values, exceeding 36 °C, compared with approximately 34 °C in Klaipėda. At both locations, heat-stress days became more frequent after 2000, particularly during 2010–2025, alongside pronounced interannual variability.

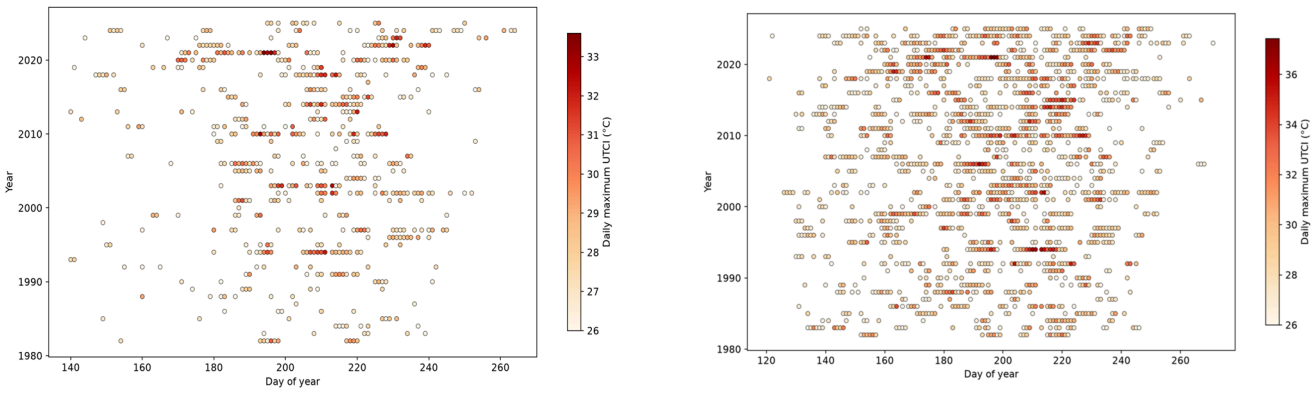

(**a**) (**b**)

Figure 9. Strip plot of individual heat-stress days near (**a**) Klaipėda and (**b**) Vilnius, based on Copernicus data during the warm season (May–September), 1982–2025. Each point represents one heat-stress day (UTCI ≥ 26 °C), plotted by its date within the season (x-axis) and year (y-axis), illustrating the temporal distribution and interannual variability of heat-stress occurrence.

The UTCI analysis shows changes in modeled thermophysiological heat stress at Klaipėda and Vilnius over the 44-year period from 1982 to 2025 (Figures 10 and 11). Moderate heat-stress days (26 ≤ UTCI < 32 °C) predominated in both cities but were substantially more frequent in Vilnius. The total annual number of UTCI heat-stress days ranged from 11 to 73 in Vilnius and from 1 to 27 in Klaipėda. Strong heat stress (32 ≤ UTCI < 38 °C)

occurred in Vilnius in many years, whereas in Klaipėda it was limited to isolated days. No days with very strong or extreme heat stress (UTCI ≥ 38 °C) were identified in either city. Years with higher numbers of UTCI heat-stress days became more frequent in the latter part of the study period, particularly in Vilnius.

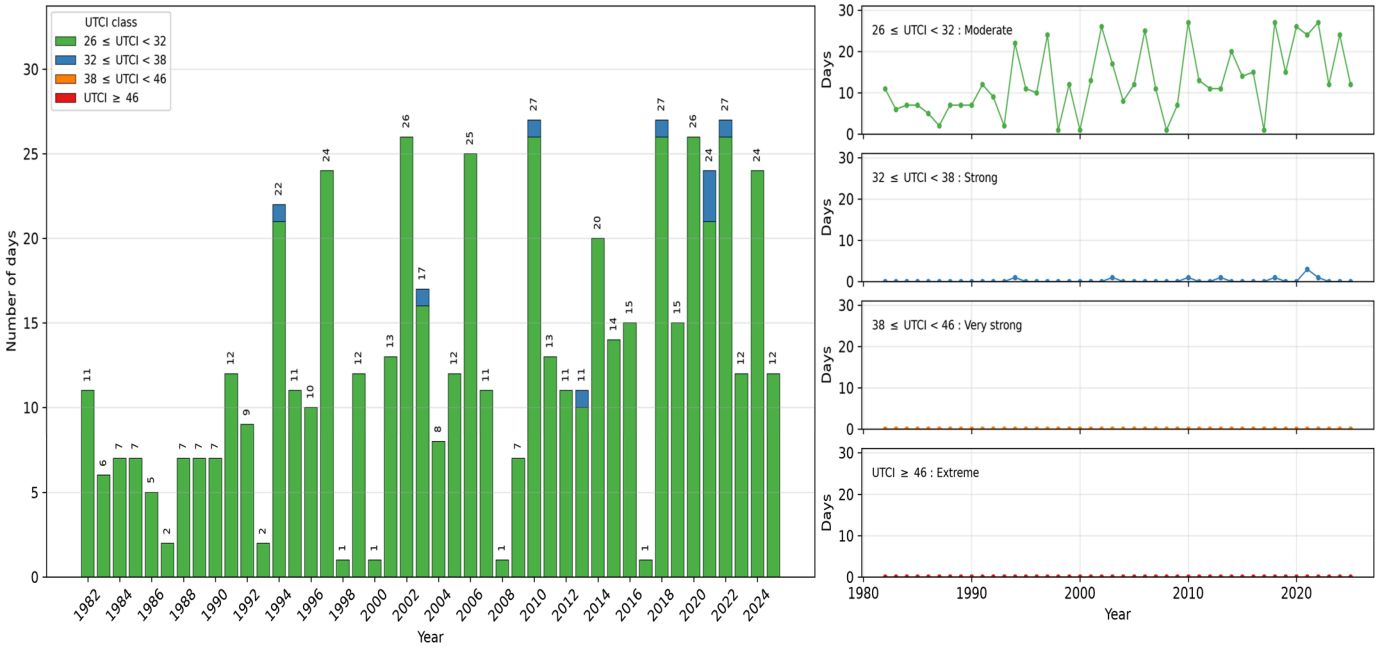

Figure 10. Annual number of days by daily maximum UTCI stress class in the ERA5-HEAT grid cell representing Klaipėda during May–September (1982–2025). The left panel shows the number of days per year, grouped into four UTCI categories: moderate (26 to <32 °C), strong (32 to <38 °C), very strong (38 to <46 °C), and extreme (≥46 °C). The right-hand panels show annual counts for each UTCI stress category.

During the research period (1982–2025), 553 moderate and 9 strong UTCI heat-stress days were recorded in Klaipėda. In Vilnius, moderate heat-stress days were nearly three times as frequent, with 1434 days recorded, while strong heat-stress days were approximately nineteen times as frequent, with 174 days recorded (Figures 10 and 11).

Humidex index values provide a complementary perspective on coastal and inland heat exposure by combining air temperature and atmospheric moisture. Figure 12 shows Humidex at the hour of Tmax on days with Tmax ≥25 °C during May–September (1982–2025). Humidex exceeded the corresponding air temperature on nearly all selected days at both locations, indicating a positive humidity contribution to the index. Even when Tmax was between 25 and 30 °C, many days reached the moderate discomfort category. Thus, humidity-related discomfort occurred on days below the national 30 °C air-temperature threshold. Vilnius had more than twice as many selected days as Klaipėda (1051 and 451, respectively) and reached higher Humidex values.

Despite the difference in the absolute number of days with Tmax ≥ 25 °C, their relative distributions among Humidex categories were similar (Figure 13). The moderate discomfort category accounted for approximately 63% (284 days) in Klaipėda and 60% (627 days) in Vilnius. The little discomfort category accounted for approximately 37% (167 days) and 40% (423 days), respectively. Only one day in Vilnius reached the great discomfort category, compared with none in Klaipėda. Neither location reached the dangerous category.

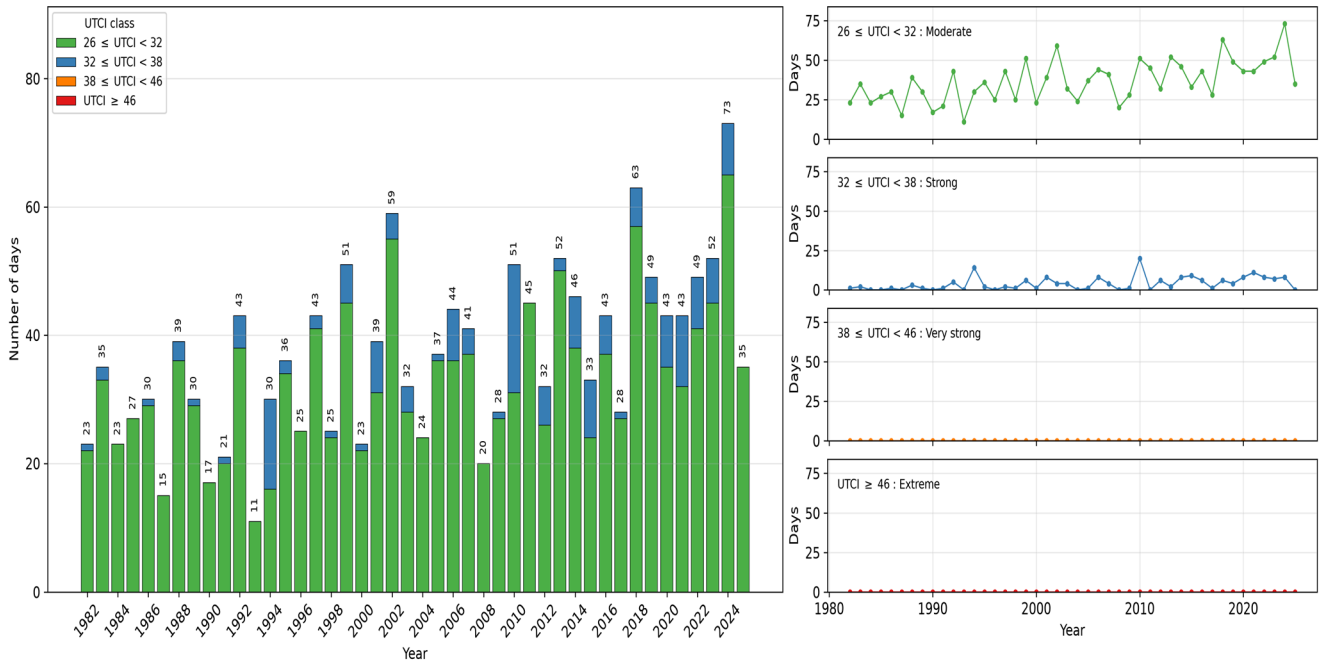

Figure 11. Annual number of days by daily maximum UTCI stress class in the ERA5-HEAT grid cell representing Vilnius during May–September, 1982–2025. The left panel shows the number of days per year, grouped into four UTCI categories: moderate (26 to <32 °C), strong (32 to <38 °C), very strong (38 to <46 °C), and extreme (≥46 °C). The right-hand panels show annual counts for each UTCI stress category.

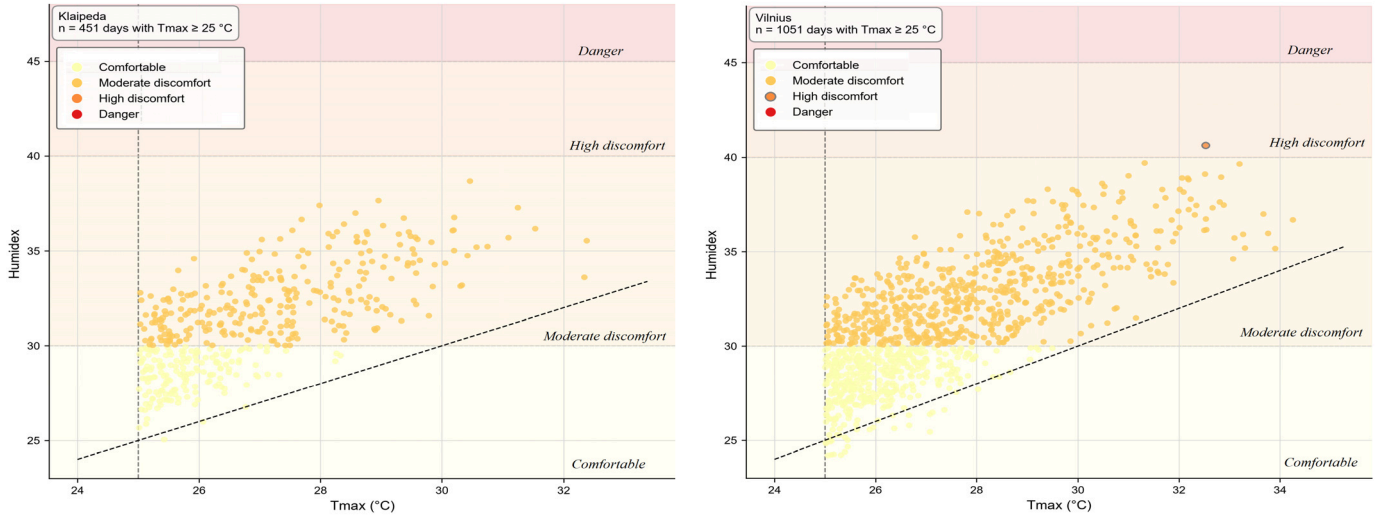

Figure 12. Relationship between daily maximum air temperature (Tmax, °C) and Humidex at the hour of Tmax (H, °C) near (**a**) Klaipėda and (**b**) Vilnius during May–September (1982–2025). Each point represents a day with Tmax ≥ 25 °C. The dashed line marks H = Tmax; points above it indicate a positive humidity contribution to Humidex.

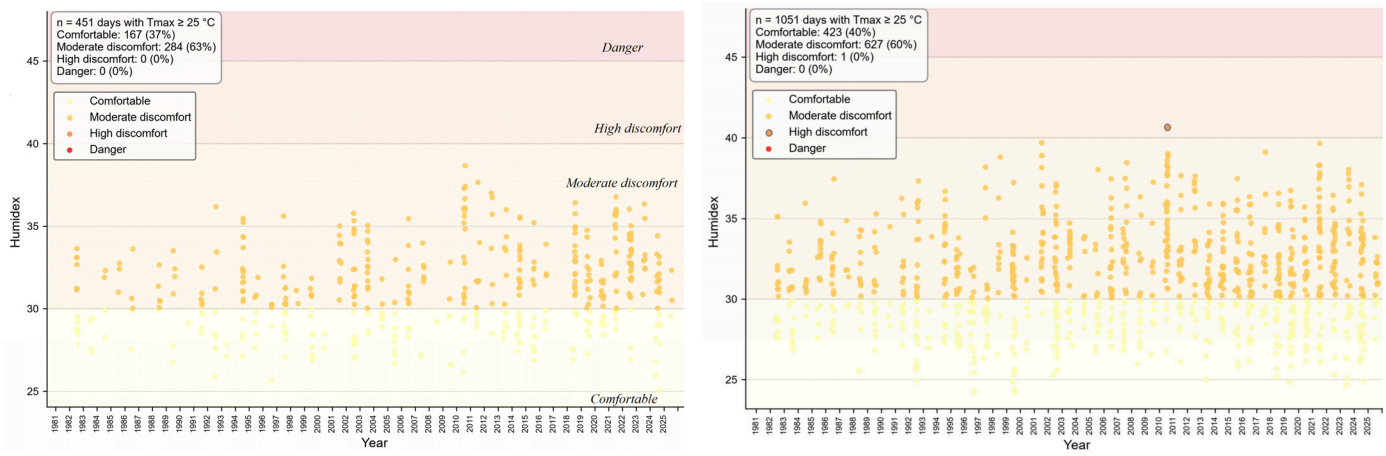

(**a**) (**b**)

Figure 13. Humidex at the hour of Tmax on days with Tmax ≥ 25 °C near (**a**) Klaipėda and (**b**) Vilnius during May–September, 1982–2025. Each point represents one selected day. Shaded bands indicate the Humidex categories defined in Section 2. Insets report category counts and percentages relative to all selected days at each location (451 in Klaipėda and 1051 in Vilnius).

The annual number of days reaching at least moderate discomfort (Humidex ≥ 30 at the hour of Tmax) increased at both locations during May–September, 1982–2025, alongside pronounced interannual variability (Figure 14). This analysis included days with Tmax below 25 °C. The linear trend was +0.27 days per year in Klaipėda ($R^2 = 0.27$) and +0.37 days per year in Vilnius ($R^2 = 0.30$). Mean annual counts increased from 3.0 in 1982–1991 to 12.3 in 2016–2025 in Klaipėda (+9.3 days), and from 8.5 to 21.3 in Vilnius (+12.8 days). The larger increase occurred in Vilnius. At both locations, the increase was mainly associated with days in the Humidex moderate discomfort category.

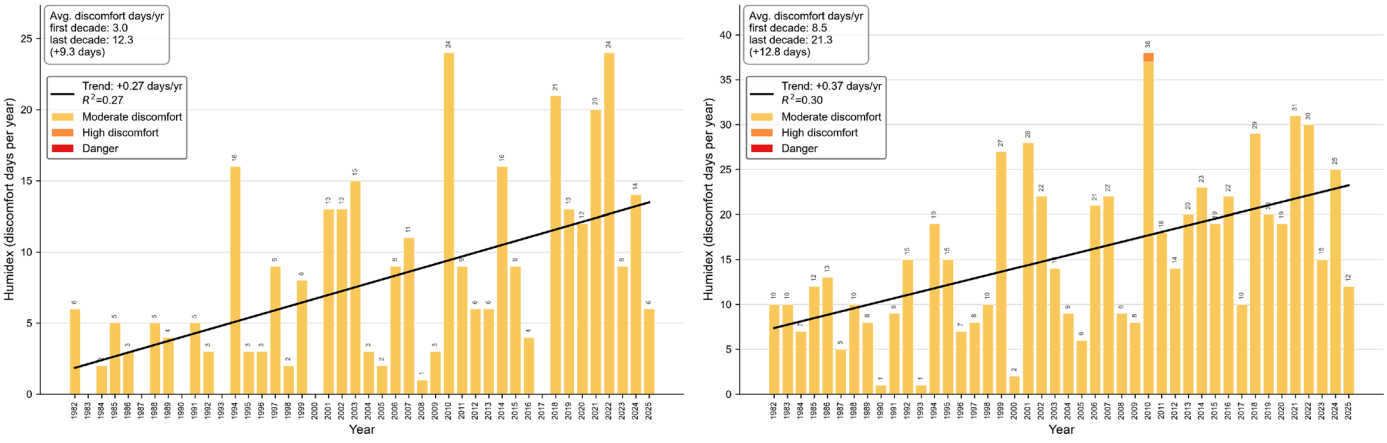

(**a**) (**b**)

Figure 14. Annual number and long-term linear trend of Humidex discomfort days near (**a**) Klaipėda and (**b**) Vilnius during May–September, 1982–2025. Days with Humidex ≥ 30 at the hour of Tmax were counted without a Tmax ≥25 °C restriction. Solid lines show linear trends.

The trends were statistically significant using Newey–West standard errors, which account for temporal dependence and unequal residual variance. The corresponding 95% confidence intervals for the slopes were 0.16–0.38 days per year in Klaipėda and 0.25–0.49 days per year in Vilnius (both $p < 0.001$). Using daily maximum Humidex increased the total number of discomfort days during 1982–2025 from 337 to 352 in Klaipėda and from 673 to 691 in Vilnius. The corresponding trends were +0.28 and +0.37 days per year, re-

spectively, closely matching those obtained using Humidex at the hour of Tmax. These Humidex findings were consistent with the UTCI results for days with at least moderate heat stress (UTCI ≥ 26 °C), with both indices showing larger estimated increases in Vilnius than in Klaipėda.

To examine whether the same coastal–inland pattern was evident at night, meteorological station observations of tropical nights (Tmin ≥ 20 °C) were analysed as an indicator of limited nocturnal cooling. During May–September, 1982–2025, tropical nights averaged 1.45 per year in Klaipėda and 0.61 in Vilnius, increasing to 2.6 and 0.9, respectively, during 2016–2025. Unlike the daytime UTCI and Humidex threshold exceedances, tropical nights were more frequent in Klaipėda (Figure 15). Their annual frequency increased by 0.76 nights per decade in Klaipėda and 0.29 nights per decade in Vilnius.

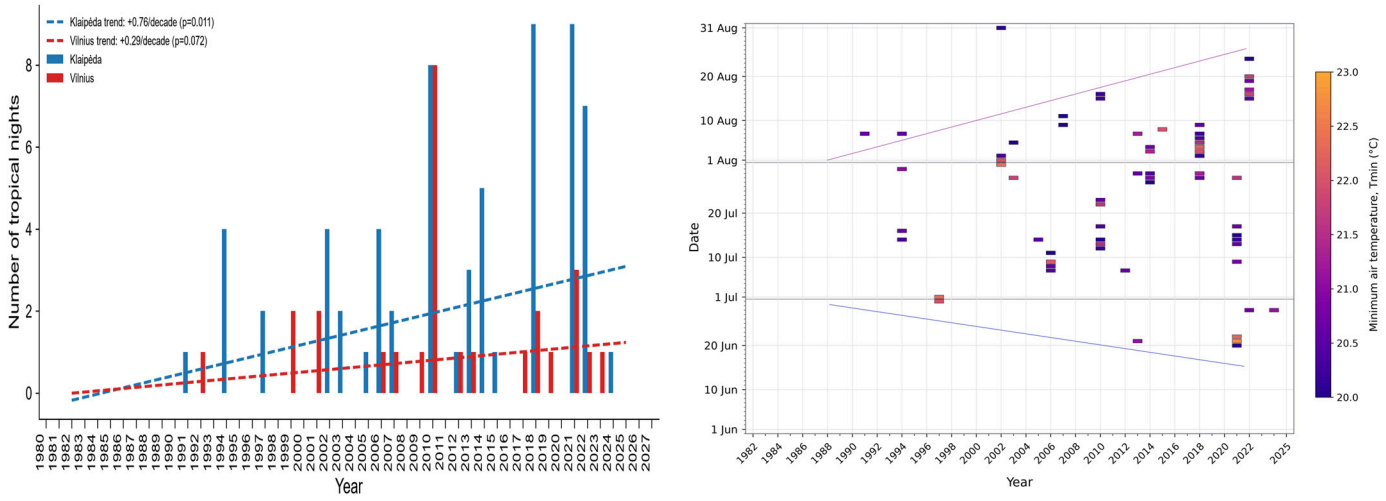

(**a**) (**b**)

Figure 15. (**a**) Annual number of tropical nights (Tmin ≥20 °C) at Klaipėda and Vilnius during May–September, 1982–2025, based on in situ observations. The *p*-values shown in the legend are from conventional OLS tests. (**b**) Seasonal timing of tropical nights (daily Tmin ≥ 20 °C) at Klaipėda.

Using Newey–West standard errors, the corresponding 95% confidence intervals were 0.31–1.21 nights per decade in Klaipėda ($p = 0.002$) and 0.07–0.50 nights per decade in Vilnius ($p = 0.009$). The estimated rates of increase were unchanged. The increase in Klaipėda was statistically significant under both the conventional OLS and Newey–West assessments, whereas in Vilnius it was statistically significant only under the Newey–West assessment (conventional OLS $p = 0.072$). The Newey–West assessment allows for unequal residual variance and possible temporal dependence when testing the same estimated trend. For Vilnius, the slope standard error was 0.0156 nights per year under conventional OLS and 0.0106 under Newey–West estimation. The smaller standard error accounts for the lower *p*-value. The maximum Newey–West lag was varied from one to five years to check whether the conclusion depended on the three-year choice. Both positive trends remained statistically significant throughout this check. For Vilnius, *p*-values ranged from 0.0053 to 0.0122. In Klaipėda, the Ljung–Box test also indicated temporal dependence in the regression residuals through lag 4 ($p = 0.002$). These results indicate a long-term increase in tropical-night frequency at both stations, with a larger estimated rate of increase in Klaipėda than in Vilnius.

In Klaipėda, tropical nights occurred both individually and in sequences of consecutive nights. It should be noted that tropical nights were a very rare phenomenon in Lithuania (Figure 15). Within the 1982–2025 study period, the first event in Klaipėda was recorded only in 1991. Tropical nights usually occur in July and August, but over the last month

earlier (Figure 15b). During the research period, 64 tropical nights were recorded across 39 episodes (Figure 15b). Most episodes lasted one night (25 episodes; 64%), while six lasted two nights, seven lasted three nights, and one lasted six consecutive nights. The longest episode occurred on 2–7 August 2018. The proportion of episodes lasting at least two consecutive nights increased from 20% in 1982–2003 (2 of 10 episodes) to 41% in 2004–2025 (12 of 29 episodes). The annual maximum duration of tropical-night episodes increased by 0.38 nights per decade (Newey–West 95% CI: 0.19–0.57; $p < 0.001$; lag 4). Alongside the increase in tropical-night frequency, this trend indicates that the longest annual sequences of warm nights became longer in Klaipėda.

The comparison of daytime and nighttime temperatures showed that all recorded tropical nights coincided with days when Tmax was ≥25 °C, although not all days reaching this threshold were associated with tropical nights. These findings indicate that compound events combining consecutive days with elevated daytime temperatures and tropical nights have become more frequent and prolonged in Lithuania, as illustrated by the Klaipėda record. Differences between the coastal and inland locations may reflect the specific characteristics of the coastal maritime climate.

Together, the daytime and night-time results show different coastal and inland patterns: UTCI and Humidex threshold exceedances were more frequent in Vilnius, whereas tropical nights were more frequent in Klaipėda. Over the same study period, Klaipėda recorded more than twice as many tropical nights as Vilnius (64 and 27, respectively). The following section extends this analysis to the spatial distribution of high-temperature conditions across Lithuania using a percentile-based approach.

3.5. Spatial Distribution of Extreme Tmax Based on the 90th Percentile

While UTCI and Humidex characterize heat stress by integrating temperature with other meteorological variables relevant to human thermal comfort, the spatial distribution of Tmax provides an additional perspective on the geographical variability of extreme heat conditions. Therefore, the following analysis examines the 90th percentile of Tmax and its spatial distribution across Lithuania, allowing regional differences in high-temperature conditions to be identified. This spatial assessment includes both locally relative Tmax percentiles and fixed-threshold hot days, heatwave occurrence and the magnitude of threshold exceedance.

The 90th percentile values of Tmax were calculated for each grid cell in the study area using Tmax data for the entire warm season (May–September) over the study period (1982–2025). The spatial distribution of 90th percentile values across Lithuania was then assessed. This approach complements the fixed 30 °C threshold by identifying locally high temperatures relative to the warm-season distribution in each grid cell. The spatial distribution of the 90th percentile values clearly reflects the influence of both continental and maritime climates. The highest values (25.5–26.0 °C) were calculated in the southern, south-western, and central parts of the country, which are characterised by a continental climate. In contrast, the lowest 90th percentile values (21–22 °C) occur along the coast, where the maritime climate predominates (Figure 16). These percentile thresholds describe locally high temperatures relative to the warm-season climate of each grid cell.

To assess how the reference period influenced the percentile thresholds, an additional comparison was performed using station Tmax observations from Klaipėda and Vilnius. Using the full 1982–2025 warm-season record, the 90th-percentile thresholds were 25.6 °C in Klaipėda and 27.3 °C in Vilnius. The corresponding thresholds were 25.0 °C and 26.9 °C using the 1982–2011 reference period, and 25.9 °C and 27.5 °C using 1991–2020. The threshold remained lower in Klaipėda under all three reference periods.

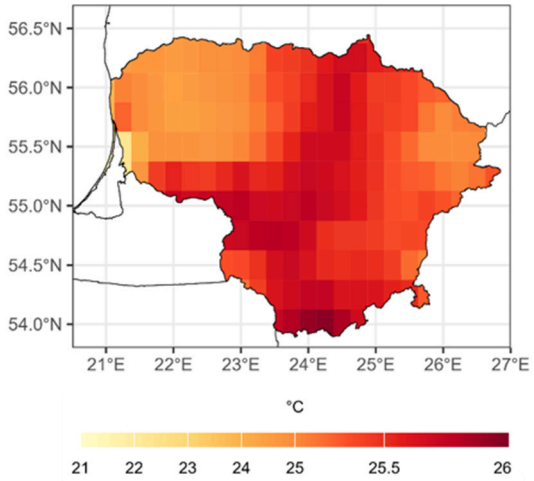

Figure 16. Distribution of the 90th percentile values of maximum daily air temperature in Lithuania over 1982–2025. The percentile values were calculated for the whole warm season (May–September).

The spatial patterns of the gridded 90th-percentile Tmax values may also reflect differences in topography, land cover, and soil moisture. Higher values of the warm-season Tmax 90th percentile generally occurred in lowlands and plains, whereas lower values were observed in upland areas. Reduced soil moisture could favour higher air temperatures by limiting evaporative cooling, potentially contributing to the higher percentile values in southern Lithuania. Although westerly airflow predominates over Lithuania, southerly advection can bring hot tropical air masses during the warm season [59], further contributing to episodes of elevated air temperature.

During 1991–2020, the highest number of hot days (2.4–2.6 days per year) was also calculated in the southernmost part of Lithuania (Figure 17a). This is also the part of Lithuania where the highest number of hot days was found in the study by Jaagus et al. (2024) [44]. In this case, clear differences can likewise be observed between the maritime climate of western Lithuania and the continental climate of the southern part of the country. While the highest number of hot days occurred in southern Lithuania, no hot days were identified at all in some grid cells along the Lithuanian coast.

To assess changes in the recurrence of hot days in Lithuania, the number of such days at the beginning (1982–2001) and end (2006–2025) of the study period was compared. The spatial distribution of hot days was similar in both the first and last 20-year periods of the study: the highest numbers were observed in the southern and south-western parts of the country, while the lowest occurred in western Lithuania (Figure 17b,c). However, it should be noted that ERA5 data are provided as grid cell values representing areal averages over about 0.25° × 0.25°. In coastal cells that include both land and sea, this can lead to a reduction in the daily maximum air temperature values. Therefore, some indicators (e.g., the number of hot days or heatwaves) are expected to be underestimated there relative to land stations. The maps produced in this study are used to describe large-scale patterns.

The number of hot days increased across all of Lithuania. Statistically significant changes ($p < 0.05$) were found in 70% of the study area. After the FDR adjustment, this number was reduced to 67% of grid cells, meaning that the correction did not substantially change the spatial pattern. The largest increases, reaching 2.0–2.4 additional hot days per year, were calculated in the south-western and southern parts of Lithuania (Figure 17d). Thus, the number of hot days has increased most markedly in the part of Lithuania where this phenomenon was already frequent.

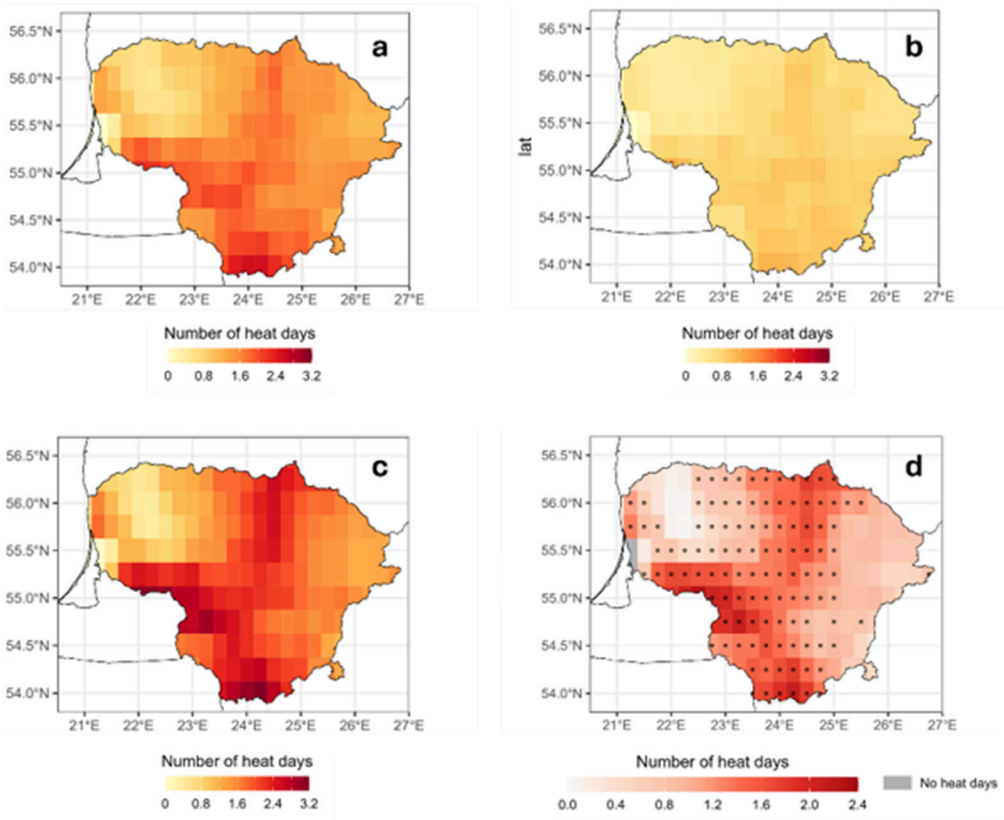

Figure 17. Mean annual number of hot days during (**a**) the 1991–2020 standard climate normal period, (**b**) 1982–2001, and (**c**) 2006–2025; (**d**) the change in the mean annual number of hot days between the latter two periods (2006–2025 minus 1982–2001). A hot day is defined as a day with a daily maximum air temperature ≥ 30 °C. Dots in panel (**d**) indicate grid cells with statistically significant differences between the two periods according to the Mann–Whitney–Wilcoxon test ($p < 0.05$) after Benjamini–Hochberg FDR adjustment.

The spatial distribution of heatwaves, defined as at least three consecutive days with Tmax ≥ 30 °C, was also examined. This temperature–duration criterion corresponds to the Lithuanian classification as a severe meteorological phenomenon [15]. Heatwave occurrence was spatially uneven (Figure 18), with the highest totals in southern Lithuania, where approximately 12–14 events were identified during May–September over 1982–2025. The deviations of Tmax from the 30 °C threshold during hot days were also assessed. The results showed that, during 1991–2020, the largest deviations (1.40–1.53 °C) were characteristic of southern Lithuania (Figure 19a). Thus, in this part of the country, hot days were frequent and their conditional mean Tmax excess was greatest. We also note that not a single grid cell showed a statistically significant change after Benjamini–Hochberg FDR adjustment at the 0.05 level.

At the beginning of the study period (1982–2001), the largest mean Tmax exceedances above 30 °C occurred in southern and north-western Lithuania, ranging from 1.53 to 1.64 °C (Figure 19b). During the last 20 years of the study period, the largest mean exceedances occurred in southern Lithuania and ranged from 1.44 to 1.54 °C (Figure 19c). Although the number of hot days increased across Lithuania, the mean exceedance decreased slightly in 90.6% of the study area (Figure 19d).

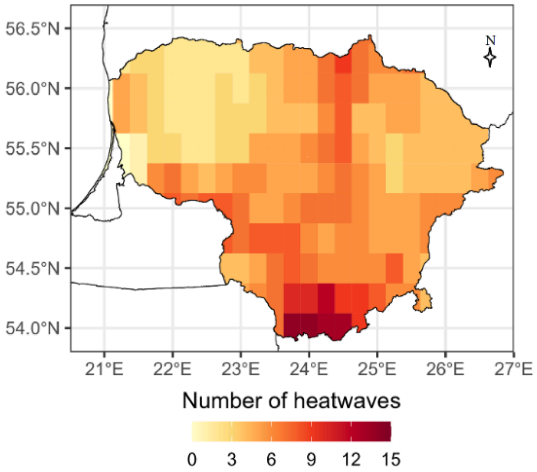

Figure 18. Number of heatwaves (when the daily maximum air temperature is ≥30 °C for at least 3 consecutive days) in Lithuania in 1982–2025.

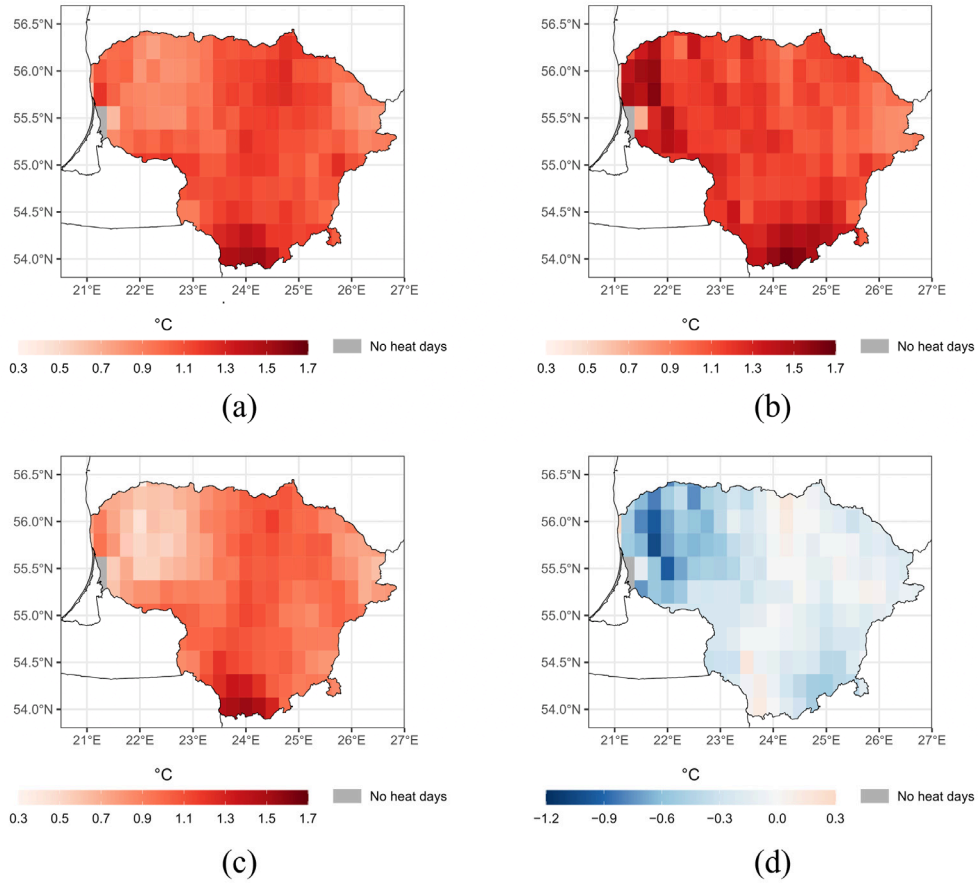

Figure 19. Mean deviation of maximum air temperature from the 30 °C threshold on hot days during the standard climate normal period of 1991–2020 (**a**), 1982–2001 (**b**), 2006–2025 (**c**), and the difference in deviations obtained by comparing the 2006–2025 and 1982–2001 periods (**d**).

4. Discussion and Recommendations

As climate change intensifies extreme heat events in the 21st century, understanding regional differences and long-term changes in heat exposure is becoming increasingly important. However, selecting a single index that adequately represents heat stress across different climatic settings remains challenging because assessment criteria vary and populations differ in their adaptation to prevailing climatic conditions. Even within the relatively

small territory of Lithuania, changes in hot days and tropical nights differ between areas influenced by maritime and continental climates. This study therefore assessed long-term changes in heat stress, hot days and tropical nights in Lithuania using Copernicus ERA5 and ERA5-HEAT data, the UTCI and Humidex indices, and national criteria for heat-related meteorological hazards.

Heat extremes have intensified worldwide, with more frequent hot days, warm nights and heatwaves [1,4,5]. This global change also includes more heat-stress days and tropical nights, while compound daytime–nighttime heat events have become more common and longer across all continents [60]. In this study, we show a similar development in Lithuania: daytime heat stress and tropical nights became more frequent at both stations, and the longest annual tropical-night sequences lengthened in Klaipėda. Importantly, all recorded tropical nights in Klaipėda coincided with days with Tmax $\geq$ 25 °C. Such compound events, combining warm days with repeated warm nights, can prolong heat stress and limit the body's opportunity to recover from daytime heat, even during the night [60,61].

The results showed a clear coastal–inland contrast between daytime and nighttime conditions. UTCI and Humidex threshold exceedances were more frequent in Vilnius, whereas tropical nights were more frequent in Klaipėda. These findings extend earlier coastal research [28,35] by comparing daytime thermal stress and nighttime temperatures at two locations approximately 300 km apart. Mapping the spatial distribution of the 90th-percentile Tmax values further revealed regional differences, with lower thresholds along the coast and higher thresholds in southern, south-western and central Lithuania.

Increasing hot-day frequency across Lithuania indicates a growing need to incorporate heat exposure into public-health protection and sustainable regional planning. This development agrees with Jaagus et al. [44] (2024), who found that the number of extremely warm days (Tmax > 27 °C) approximately doubled across the eastern Baltic region during 1951–2021. Their study also identified fewer such days along the coast and more in southern and continental areas. Our results show a similar increase and geographical pattern, while extending the assessment to different thermal-stress categories and nighttime conditions. Jaagus et al. [44] (2024) also found stronger increases in heatwave-day frequency than in heatwave temperature-anomaly measures. Although the indicators differ, both studies show that changes in frequency and temperature exceedance need to be distinguished: in our analysis, hot days became more frequent while their mean Tmax exceedance above 30 °C decreased slightly across most of Lithuania.

A contribution of this study is the application of Copernicus ERA5-HEAT UTCI data to assess long-term changes in thermal-stress categories in Lithuania alongside national temperature criteria. Combined with station observations, Copernicus data could support regional heat-stress assessment, spatial planning and climatological baselines for warning systems, including areas between meteorological stations. Along the coastline, station observations remain particularly important: reanalysis does not capture all locally observed Tmax $\geq$ 30 °C days, consistent with earlier Lithuanian coastal research [28].

Moderate and strong UTCI heat stress occurred in the analysed records, whereas the higher categories were absent. Nevertheless, heatwaves meeting the Lithuanian criterion of Tmax $\geq$ 30 °C for at least three consecutive days were recorded at both locations [14,15]. This difference reflects the distinct definitions: UTCI describes thermal stress using several meteorological variables, while the national criterion identifies persistent high air temperatures. The mapped warm-season Tmax 90th-percentile values provide additional local climatic context, ranging from approximately 21 °C near the coast to 26 °C inland. Temperatures below the fixed 30 °C threshold can therefore be unusually high for the local climate. Comparison with other European climates further clarifies the Lithuanian results. Tomczyk and Katragkou [48] (2025) found that slight Humidex discomfort predominated

during heatwaves in Poznań, whereas Thessaloniki experienced substantial proportions of significant and dangerous discomfort. These differences show that heatwaves can be associated with different levels of thermal discomfort across climatic regions. For Lithuania, the discomfort recorded below 30 °C supports including Humidex information in public advice on hot weather even when the national heatwave criterion is not met.

The health relevance of thermal conditions also varies with the regional climate. Di Napoli et al. [62,63] (2018, 2019) found that the relationship between UTCI and mortality varied with European bioclimatic conditions. More directly, Sánchez Martínez et al. [13] (2018) identified increased summer mortality in Vilnius from Tmax = 30 °C during 2009–2015, estimating approximately seven heat-related deaths annually. Their future projections differed substantially depending on assumed acclimatisation, showing the influence of these assumptions on projected health outcomes. These findings support the development of locally informed protective measures, including for temperatures below those associated with the highest thermal-stress categories.

The increasing frequency of daytime heat stress and discomfort at both locations strengthens the need for heat protection throughout the warm season. Importantly, the increases were mainly associated with moderate UTCI heat stress and Humidex discomfort, indicating that adaptation should address recurring thermal stress alongside the most intense heat episodes. Forecasts of UTCI and Humidex, high air temperatures and tropical nights could be used together to communicate the expected severity and duration of heat. Such information could help municipalities and health services tailor advice and assistance to older people, children, people with chronic illnesses and outdoor workers [61].

The coastal findings also show why nighttime conditions matter for adaptation in buildings. In Klaipėda, the proportion of tropical-night episodes lasting at least two nights increased from 20% in 1982–2003 to 41% in 2004–2025. These longer sequences can restrict opportunities to remove stored indoor heat overnight. European analyses by Artmann et al. showed that nighttime ventilation depends on the temperature difference between the building interior and outdoor air, and that warming reduces this cooling potential [64,65]. Our findings therefore support including summer overheating in building design and renovation alongside winter heat conservation [66]. External shading, insulation and controllable ventilation should consequently be considered together when selecting measures to reduce overheating [67]. Lithuanian evidence further shows why thermal comfort and indoor air quality need to be addressed jointly: Leivo et al. found lower ventilation rates and higher carbon dioxide concentrations after energy retrofits in the Lithuanian buildings they studied [68]. The warm-season temperature range of 18–28 °C specified by Lithuanian Hygiene Norm HN 42:2009 for residential rooms and visitor areas in public buildings provides an existing national reference for assessing indoor conditions [69]. Where passive measures are insufficient, efficient cooling may be needed, with equipment efficiency helping to limit electricity use and household costs [70].

The higher frequency of hot days in southern and inland Lithuania provides a spatial basis for prioritising protection in public spaces. Shade and access to drinking water are particularly important along pedestrian routes and in places where people wait or remain outdoors for longer periods [61]. Their surroundings also influence thermal conditions: street geometry and heat-storing surfaces affect airflow and radiant exposure [71,72]. Trees and shade canopies should therefore provide shade while retaining ventilation. Surface materials also require attention, because highly reflective paving can reduce air temperature while increasing the radiant heat load experienced by pedestrians [73]. Land-cover information could help municipalities apply these regional priorities locally. Schwaab et al. found greater summer surface cooling associated with trees than with treeless green spaces in European cities [74]. This finding supports considering vegetation type as well as the

extent of green space. Combining tree-canopy, NDVI, albedo and land-use information with local assessments of shade and airflow could help identify exposed pedestrian areas where additional trees or shading structures would be most useful.

Future research should link the complementary thermal-stress indicators used in this study—UTCI, Humidex and tropical-night frequency—to daily morbidity, hospital admissions, ambulance calls and mortality, distinguishing age groups, chronic conditions and delayed effects. Building on the UTCI–mortality relationships examined by Di Napoli et al. [62,63] and the temperature–mortality findings for Vilnius reported by Sánchez Martínez et al. [13], this would help assess whether considering daytime thermal stress together with nighttime conditions improves the basis for Lithuanian heat warnings. The pilot spectra provide a further research direction: the similar timescales of Tmax variability identified at Klaipėda and Vilnius could be examined across a wider station network. Comparisons with atmospheric circulation indices and Baltic Sea surface temperatures could then help investigate regional patterns of temperature variability alongside the observed long-term increases in heat exposure.

Overall, our results reveal long-term increases in heat stress in Lithuania, where heat events are concentrated in the warm season. Importantly, populations accustomed to lower temperatures can experience heat-related health risks even where the highest thermal-stress categories are uncommon [11–13,62,63]. Daytime heat stress and tropical nights became more frequent at both locations, while the longest annual tropical-night sequences lengthened in Klaipėda. These findings are consistent with the global intensification of heat stress, which poses growing challenges to health, livelihoods and economic productivity [60]. Our results therefore support including both daytime thermal stress and nighttime heat in public-health protection, climate adaptation and regional planning in Lithuania.

5. Conclusions

The analysis of Copernicus ERA5 and ERA5-HEAT data together with meteorological station observations showed increasing heat exposure in Lithuania during 1982–2025, with distinct coastal–inland differences in daytime and nighttime conditions. UTCI, Humidex, and national temperature criteria provided complementary information on these changes.

Mapping the spatial distribution of the warm-season Tmax 90th percentile using ERA5 data revealed lower values along the coast, approximately 21–22 °C, and higher values in southern, southwestern and central Lithuania, reaching 25.5–26.0 °C. A comparison of two equal 20-year periods, 1982–2001 and 2006–2025, showed an increase in the number of hot days with Tmax $\geq$ 30 °C, with the greatest increases in southern and southwestern inland areas. This increase was statistically significant in 67% of the analysed grid cells after FDR adjustment.

Based on observations from the Klaipėda and Vilnius meteorological stations, heatwaves meeting Lithuania's national severe-event criterion (Tmax $\geq$ 30 °C for at least three consecutive days) increased between 1982–2001 and 2006–2025 from 1 to 10 in Klaipėda and from 5 to 16 in Vilnius. Heatwave days increased from 3 to 35 and from 23 to 66, respectively. These results indicate more frequent episodes of persistent extreme heat at both locations, with more heatwave events and days in Vilnius.

The ERA5-HEAT UTCI and ERA5-derived Humidex results showed more frequent daytime heat stress and discomfort in Vilnius than in Klaipėda. The annual number of days with UTCI $\geq$ 26 °C increased by approximately 3 days per decade in Klaipėda and 6 days per decade in Vilnius. For Humidex $\geq$ 30 evaluated at the hour of Tmax, the corresponding increases were 2.7 and 3.7 days per decade. Moderate heat stress and moderate discomfort predominated in the respective UTCI and Humidex analyses.

Station observations showed a different coastal–inland pattern for tropical nights, when Tmin ≥ 20 °C. Tropical nights were more frequent in Klaipėda, and their annual number increased by 0.76 nights per decade, compared with 0.29 nights per decade in Vilnius. Thus, while daytime heat stress and discomfort were more frequent and increased more rapidly in Vilnius, tropical nights were more frequent and increased more rapidly in Klaipėda.

Copernicus ERA5 and ERA5-HEAT data complemented station observations in assessing regional heat exposure. However, ERA5 did not capture all locally observed Tmax ≥ 30 °C days, particularly along the coast, demonstrating the importance of station measurements for identifying local temperature extremes.

An exploratory spectral comparison, covering all 528 calendar months during 1982–2025, identified similar 2–3-year timescales of maximum air temperature variability at both locations, although their pointwise statistical support differed.

The complementary use of UTCI, Humidex and tropical-night frequency distinguished daytime thermal stress, temperature–humidity discomfort and nighttime heat exposure. These findings could inform geographically differentiated climate adaptation planning, with attention to daytime heat stress in inland areas and warm nighttime conditions along the coast.

Author Contributions: Conceptualization, I.D., L.K., R.D., and D.V.; methodology, I.D., D.V., L.K., M.R., R.D., and A.N.; software, L.K., A.N., R.D., and M.R.; validation, I.D., M.R., A.N., L.K., D.V., and R.D.; formal analysis, I.D., L.K., D.V., M.R., R.D., R.G., A.N., and B.P.; investigation, I.D., L.K., M.R., A.N., R.D., D.V., and B.P.; resources, D.V., M.R., L.K., and I.D.; data curation, I.D., D.V., L.K., A.N., R.D., and M.R.; writing—original draft preparation, I.D., L.K., M.R., A.N., R.D., D.V., R.G., and B.P.; writing—review and editing, I.D., L.K., R.D., A.N., and B.P.; visualization, I.D., M.R., L.K., A.N., and R.D.; supervision, I.D. All authors have read and agreed to the published version of the manuscript.

Funding: This research received no external funding.

Institutional Review Board Statement: Not applicable. The study analyses meteorological observations and reanalysis data and does not involve human participants or animals.

Informed Consent Statement: Not applicable.

Data Availability Statement: ERA5 and ERA5-HEAT data are publicly available from the Copernicus Climate Change Service Climate Data Store under the dataset citations provided in the References. Station observations are available through the Lithuanian Hydrometeorological Service (LHMT), subject to the provider's access conditions. The derived datasets and analysis code used in this study are available from the corresponding author upon reasonable request.

Conflicts of Interest: The authors declare no conflicts of interest.

References

1. IPCC. *Climate Change 2021: The Physical Science Basis*; Cambridge University Press: Cambridge, UK; New York, NY, USA, 2021. [CrossRef]
2. Jendritzky, G.; de Dear, R.; Havenith, G. UTCI-Why Another Thermal Index? *Int. J. Biometeorol.* **2012**, *56*, 421–428. [CrossRef] [PubMed]
3. World Meteorological Organization; World Health Organization. *Heatwaves and Health: Guidance on Warning-System Development*; WMO-No. 1142; World Meteorological Organization: Geneva, Switzerland, 2015. Available online: https://www.who.int/docs/default-source/climate-change/heat-waves-and-health—guidance-on-warning-system-development.pdf (accessed on 16 August 2026).
4. Seneviratne, S.I.; Zhang, X.; Adnan, M.; Badi, W.; Dereczynski, C.; Di Luca, A.; Ghosh, S.; Iskander, I.; Kossin, J.; Lewis, S.; et al. Weather and Climate Extreme Events in a Changing Climate. In *Climate Change 2021: The Physical Science Basis*; Masson-Delmotte, V., Zhai, P., Pirani, A., et al., Eds.; Cambridge University Press: Cambridge, UK, 2021; pp. 1513–1766. [CrossRef]
5. Perkins-Kirkpatrick, S.E.; Lewis, S.C. Increasing Trends in Regional Heatwaves. *Nat. Commun.* **2020**, *11*, 3357. [CrossRef] [PubMed]
6. Perkins, S.E.; Alexander, L.V. On the Measurement of Heat Waves. *J. Clim.* **2013**, *26*, 4500–4517. [CrossRef]

7. Zscheischler, J.; Westra, S.; van den Hurk, B.J.J.M.; Seneviratne, S.I.; Ward, P.J.; Pitman, A.; AghaKouchak, A.; Bresch, D.N.; Leonard, M.; Wahl, T.; et al. Future Climate Risk from Compound Events. *Nat. Clim. Change* **2018**, *8*, 469–477. [CrossRef]
8. Ridder, N.N.; Pitman, A.J.; Westra, S.; Ukkola, A.; Do, H.X.; Bador, M.; Hirsch, A.L.; Evans, J.P.; Di Luca, A.; Zscheischler, J. Global Hotspots for the Occurrence of Compound Events. *Nat. Commun.* **2020**, *11*, 5956. [CrossRef] [PubMed]
9. Raymond, C.; Matthews, T.; Horton, R.M. The Emergence of Heat and Humidity Too Severe for Human Tolerance. *Sci. Adv.* **2020**, *6*, eaaw1838. [CrossRef] [PubMed]
10. Vicedo-Cabrera, A.M.; Scovronick, N.; Sera, F.; Royé, D.; Schneider, R.; Tobias, A.; Astrom, C.; Guo, Y.; Honda, Y.; Hondula, D.M.; et al. The Burden of Heat-Related Mortality Attributable to Recent Human-Induced Climate Change. *Nat. Clim. Change* **2021**, *11*, 492–500. [CrossRef] [PubMed]
11. Keatinge, W.R.; Donaldson, G.C.; Cordioli, E.; Martinelli, M.; Kunst, A.E.; Mackenbach, J.P.; Näyhä, S.; Vuori, I. Heat Related Mortality in Warm and Cold Regions of Europe: Observational Study. *BMJ* **2000**, *321*, 670–673. [CrossRef] [PubMed]
12. Ruuhela, R.; Jylhä, K.; Lanki, T.; Tiittanen, P.; Matzarakis, A. Biometeorological Assessment of Mortality Related to Extreme Temperatures in Helsinki Region, Finland, 1972–2014. *Int. J. Environ. Res. Public Health* **2017**, *14*, 944. [CrossRef] [PubMed]
13. Sánchez Martínez, G.; Díaz, J.; Hooyberghs, H.; Lauwaet, D.; De Ridder, K.; Linares, C.; Carmona, R.; Ortiz, C.; Kendrovski, V.; Adamonytė, D. Cold-Related Mortality vs Heat-Related Mortality in a Changing Climate: A Case Study in Vilnius (Lithuania). *Environ. Res.* **2018**, *166*, 384–393. [CrossRef] [PubMed]
14. Approval of Indicators of Dangerous Meteorological and Hydrological Phenomena. Order No. V-42, 10 June 2025. Available online: https://www.meteo.lt/app/uploads/2026/06/PR-2025-06-10.pdf (accessed on 21 September 2026). (In Lithuanian)
15. Indicators of Severe and Catastrophic Meteorological and Hydrological Phenomena. Annex to Order No. D1-870, as amended by Order No. D1-373, 4 November 2024. Available online: https://www.meteo.lt/app/uploads/2024/11/svetainei_SR-KR-rodikliai_2024.pdf (accessed on 21 September 2026). (In Lithuanian)
16. Steadman, R.G. The Assessment of Sultriness. Part I: A Temperature-Humidity Index Based on Human Physiology and Clothing Science. *J. Appl. Meteorol.* **1979**, *18*, 861–873. [CrossRef]
17. Rothfusz, L.P. *The Heat Index Equation (or, More Than You Ever Wanted to Know About Heat Index)*; Technical Attachment SR 90–23; National Weather Service: Fort Worth, TX, USA, 1990. Available online: https://www.weather.gov/media/bgm/ta_htindx.PDF (accessed on 13 August 2026).
18. Steadman, R.G. A Universal Scale of Apparent Temperature. *J. Clim. Appl. Meteorol.* **1984**, *23*, 1674–1687. [CrossRef]
19. Masterton, J.M.; Richardson, F.A. *Humidex: A Method of Quantifying Human Discomfort Due to Excessive Heat and Humidity*; Environment Canada: Downsview, ON, Canada, 1979. Available online: https://publications.gc.ca/site/eng/9.865813/publication.html (accessed on 28 August 2026).
20. Budd, G.M. Wet-Bulb Globe Temperature (WBGT)-Its History and Its Limitations. *J. Sci. Med. Sport* **2008**, *11*, 20–32. [CrossRef] [PubMed]
21. Höppe, P. The Physiological Equivalent Temperature-A Universal Index for the Biometeorological Assessment of the Thermal Environment. *Int. J. Biometeorol.* **1999**, *43*, 71–75. [CrossRef] [PubMed]
22. Bröde, P.; Fiala, D.; Błażejczyk, K.; Holmér, I.; Jendritzky, G.; Kampmann, B.; Tinz, B.; Havenith, G. Deriving the Operational Procedure for the Universal Thermal Climate Index (UTCI). *Int. J. Biometeorol.* **2012**, *56*, 481–494. [CrossRef] [PubMed]
23. Fiala, D.; Havenith, G.; Bröde, P.; Kampmann, B.; Jendritzky, G. UTCI-Fiala Multi-Node Model of Human Heat Transfer and Temperature Regulation. *Int. J. Biometeorol.* **2012**, *56*, 429–441. [CrossRef] [PubMed]
24. Błażejczyk, K.; Epstein, Y.; Jendritzky, G.; Staiger, H.; Tinz, B. Comparison of UTCI to Selected Thermal Indices. *Int. J. Biometeorol.* **2012**, *56*, 515–535. [CrossRef] [PubMed]
25. Hersbach, H.; Bell, B.; Berrisford, P.; Hirahara, S.; Horányi, A.; Muñoz-Sabater, J.; Nicolas, J.; Peubey, C.; Radu, R.; Schepers, D.; et al. The ERA5 Global Reanalysis. *Q. J. R. Meteorol. Soc.* **2020**, *146*, 1999–2049. [CrossRef]
26. Di Napoli, C.; Barnard, C.; Prudhomme, C.; Cloke, H.L.; Pappenberger, F. ERA5-HEAT: A Global Gridded Historical Dataset of Human Thermal Comfort Indices from Climate Reanalysis. *Geosci. Data J.* **2021**, *8*, 2–10. [CrossRef]
27. Di Napoli, C.; Barnard, C.; Prudhomme, C.; Cloke, H.L.; Pappenberger, F. *Thermal Comfort Indices Derived from ERA5 Reanalysis [Dataset]*, version 1.1; Copernicus Climate Change Service Climate Data Store: Bonn, Germany, 2020. [CrossRef]
28. Dailidienė, I.; Delalande, A.; Valiukas, D.; Dailidė, R.; Narščius, A.; Dabulevičienė, T.; Tymvios, F. Investigating Warm-Season Heatwaves Along the Lithuanian Baltic Sea Coast Applying Copernicus Datasets. *Sustainability* **2025**, *17*, 10536. [CrossRef]
29. Rousi, E.; Kornhuber, K.; Beobide-Arsuaga, G.; Luo, F.; Coumou, D. Accelerated Western European Heatwave Trends Linked to More-Persistent Double Jets over Eurasia. *Nat. Commun.* **2022**, *13*, 3851. [CrossRef] [PubMed]
30. Schaller, N.; Sillmann, J.; Anstey, J.; Fischer, E.M.; Grams, C.M.; Russo, S. Influence of Blocking on Northern European and Western Russian Heatwaves in Large Climate Model Ensembles. *Environ. Res. Lett.* **2018**, *13*, 054015. [CrossRef]
31. Spensberger, C.; Madonna, E.; Boettcher, M.; Grams, C.M.; Papritz, L.; Quinting, J.F.; Röthlisberger, M.; Sprenger, M.; Zschenderlein, P. Dynamics of Concurrent and Sequential Central European and Scandinavian Heatwaves. *Q. J. R. Meteorol. Soc.* **2020**, *146*, 2998–3013. [CrossRef]

32. Liu, X.; He, B.; Guo, L.; Huang, L.; Chen, D. Similarities and Differences in the Mechanisms Causing the European Summer Heatwaves in 2003, 2010, and 2018. *Earth's Future* **2020**, *8*, e2019EF001386. [CrossRef]
33. Meier, H.E.M.; Kniebusch, M.; Dieterich, C.; Gröger, M.; Zorita, E.; Elmgren, R.; Myrberg, K.; Ahola, M.P.; Bartosova, A.; Bonsdorff, E.; et al. Climate Change in the Baltic Sea Region: A Summary. *Earth Syst. Dyn.* **2022**, *13*, 457–593. [CrossRef]
34. Kažys, J.; Stankūnavičius, G.; Rimkus, E.; Bukantis, A.; Valiukas, D. Long-Range Alternation of Extreme High Day and Night Temperatures in Lithuania. *Baltica* **2011**, *24*, 71–82.
35. Dailidienė, I.; Servaitė, I.; Dailidė, R.; Vasiliauskienė, E.; Rapolienė, L.; Povilanskas, R.; Valiukas, D. Increasing Trends of Heat Waves and Tropical Nights in Coastal Regions: The Case Study of Lithuania Seaside Cities. *Sustainability* **2023**, *15*, 14281. [CrossRef]
36. Kapilovaitė, J.; Rimkus, E. Scenario-Based Assessment of Urban Heat-Stress Risk in Vilnius, Lithuania. *Atmosphere* **2026**, *17*, 739. [CrossRef]
37. Iles, C.; Sandstad, M.; Schwingshackl, C.; Sillmann, J. Climate Extreme Indices and Heat Stress Indicators Derived from CMIP6 Global Climate Projections: Product User Guide; Copernicus Climate Change Service. 2021. Available online: https://confluence.ecmwf.int/pages/viewpage.action?pageId=253723990 (accessed on 23 September 2026).
38. European Centre for Medium-Range Weather Forecasts (ECMWF). New Parameters: Heat and Cold Indices, Mean Radiant Temperature and Globe Temperature. 2024. Available online: https://confluence.ecmwf.int/pages/viewpage.action?pageId=462912535 (accessed on 23 September 2026).
39. Hersbach, H.; Bell, B.; Berrisford, P.; Biavati, G.; Horányi, A.; Muñoz Sabater, J.; Nicolas, J.; Peubey, C.; Radu, R.; Rozum, I.; et al. *ERA5 Hourly Data on Single Levels from 1940 to Present [Data Set]*; Copernicus Climate Change Service Climate Data Store: Bonn, Germany, 2023. [CrossRef]
40. Chen, D.; Rojas, M.; Samset, B.H.; Cobb, K.; Diongue Niang, A.; Edwards, P.; Emori, S.; Faria, S.H.; Hawkins, E.; Hope, P.; et al. Framing, Context, and Methods. In *Climate Change 2021: The Physical Science Basis*; Masson-Delmotte, V., Zhai, P., Pirani, A., Connors, S.L., Péan, C., Berger, S., et al., Eds.; Cambridge University Press: Cambridge, UK; New York, NY, USA, 2021; pp. 147–286. [CrossRef]
41. Benjamini, Y.; Hochberg, Y. Controlling the False Discovery Rate: A Practical and Powerful Approach to Multiple Testing. *J. R. Stat. Soc. B* **1995**, *57*, 289–300. [CrossRef]
42. García-León, D.; Casanueva, A.; Standardi, G.; Burgstall, A.; Flouris, A.D.; Nybo, L. Current and Projected Regional Economic Impacts of Heatwaves in Europe. *Nat. Commun.* **2021**, *12*, 5807. [CrossRef] [PubMed]
43. Smid, M.; Russo, S.; Costa, A.C.; Granell, C.; Pebesma, E. Ranking European Capitals by Exposure to Heat Waves and Cold Waves. *Urban Clim.* **2019**, *27*, 388–402. [CrossRef]
44. Jaagus, J.; Rimkus, E.; Briede, A.; Sagris, V.; Aasa, A.; Kapilovaitė, J.; Sepp, M. Long-Term Changes in Heat Wave Parameters in the Eastern Baltic Region. *Theor. Appl. Climatol.* **2024**, *155*, 5053–5068. [CrossRef]
45. Kalvāne, G.; Kalvāns, A.; Briede, A. More Frequent Warm and Dry Spells along Persistent Cold and Wet Spells in the Baltics. *Theor. Appl. Climatol.* **2026**, *157*, 162. [CrossRef]
46. Klimavičius, L.; Rimkus, E. Compound Drought and Heatwave Events in the Eastern Part of the Baltic Sea Region. *Oceanologia* **2024**, *66*, 26–36. [CrossRef]
47. Sulikowska, A.; Wypych, A. Summer Temperature Extremes in Europe: How Does the Definition Affect the Results? *Theor. Appl. Climatol.* **2020**, *141*, 19–30. [CrossRef]
48. Tomczyk, A.M.; Katragkou, E. Occurrence of Heatwaves in Selected Regions of Poland and Greece and the Characteristics of Their Biometeorological Conditions. *Quaest. Geogr.* **2025**, *44*, 107–116. [CrossRef]
49. Newey, W.K.; West, K.D. A Simple, Positive Semi-Definite, Heteroskedasticity and Autocorrelation Consistent Covariance Matrix. *Econometrica* **1987**, *55*, 703–708. [CrossRef]
50. Wahl, T.; Plant, N.G. Changes in erosion and flooding risk due to long-term and cyclic oceanographic trends. *Geophys. Res. Lett.* **2015**, *42*, 2943–2950. [CrossRef]
51. Ljung, G.M.; Box, G.E.P. On a Measure of Lack of Fit in Time Series Models. *Biometrika* **1978**, *65*, 297–303. [CrossRef]
52. Welch, P.D. The use of fast Fourier transform for the estimation of power spectra: A method based on time averaging over short, modified periodograms. *IEEE Trans. Audio Electroacoust.* **1967**, *15*, 70–73. [CrossRef]
53. Weber, R.O.; Talkner, P. Spectra and correlations of climate data from days to decades. *J. Geophys. Res. Atmos.* **2001**, *106*, 20131–20144. [CrossRef]
54. Pallotta, G.; Santer, B.D. Multi-Frequency Analysis of Simulated versus Observed Variability in Tropospheric Temperature. *J. Clim.* **2020**, *33*, 10383–10402. [CrossRef]
55. Bezuglova, N.N.; Zinchenko, G.S.; Malygina, N.S.; Papina, T.S.; Barlyaeva, T.V. Response of high-mountain Altai thermal regime to climate global warming of recent decades. *Theor. Appl. Climatol.* **2012**, *110*, 595–605. [CrossRef]
56. Mann, M.E.; Lees, J.M. Robust estimation of background noise and signal detection in climatic time series. *Clim. Change* **1996**, *33*, 409–445. [CrossRef]

57. Ghil, M.; Allen, M.R.; Dettinger, M.D.; Ide, K.; Kondrashov, D.; Mann, M.E.; Robertson, A.W.; Saunders, A.; Tian, Y.; Varadi, F.; et al. Advanced spectral methods for climatic time series. *Rev. Geophys.* **2002**, *40*, 1003. [CrossRef]
58. Jena, P.; Azad, S. Interference of significant sub-decadal periodicities in Indian monsoon rainfall. *Nat. Hazards* **2024**, *120*, 12265–12278. [CrossRef]
59. Nacionalinė žemės tarnyba prie Žemės ūkio ministerijos. *Lietuvos nacionalinis atlasas: I tomas. Lietuva pasaulyje ir Europoje. Gamta ir kraštovaizdis [National Atlas of Lithuania: Volume 1. Lithuania in the World and Europe. Nature and Landscape]*; Vilniaus universitetas, Kartografijos centras: Vilnius, Lithuania, 2014. (In Lithuanian)
60. Emerton, R.; Nicolas, J.; Lombardi, A.; Di Napoli, C. Global heat stress intensification and its expanding footprint on the human population. *Nat. Clim. Change* **2026**, *16*, 989–996. [CrossRef]
61. World Health Organization Regional Office for Europe. *Heat–Health Action Plans: Guidance*, 2nd ed.; WHO Regional Office for Europe: Copenhagen, Denmark, 2026. Available online: https://www.who.int/europe/publications/i/item/9789289062930 (accessed on 22 September 2026).
62. Di Napoli, C.; Pappenberger, F.; Cloke, H.L. Assessing Heat-Related Health Risk in Europe via the Universal Thermal Climate Index (UTCI). *Int. J. Biometeorol.* **2018**, *62*, 1155–1165. [CrossRef] [PubMed]
63. Di Napoli, C.; Pappenberger, F.; Cloke, H.L. Verification of Heat Stress Thresholds for a Health-Based Heat-Wave Definition. *J. Appl. Meteorol. Climatol.* **2019**, *58*, 1177–1194. [CrossRef]
64. Artmann, N.; Manz, H.; Heiselberg, P. Climatic Potential for Passive Cooling of Buildings by Night-Time Ventilation in Europe. *Appl. Energy* **2007**, *84*, 187–201. [CrossRef]
65. Artmann, N.; Gyalistras, D.; Manz, H.; Heiselberg, P. Impact of Climate Warming on Passive Night Cooling Potential. *Build. Res. Inf.* **2008**, *36*, 111–128. [CrossRef]
66. Ministry of Environment of the Republic of Lithuania. Ilgalaikė renovacijos strategija [Long-Term Renovation Strategy]. 2021. Available online: https://am.lrv.lt/lt/veiklos-sritys-1/statyba-ir-bustas/ilgalaike-renovacijos-strategija/ (accessed on 26 October 2026). (In Lithuanian)
67. Porritt, S.M.; Cropper, P.C.; Shao, L.; Goodier, C.I. Ranking of Interventions to Reduce Dwelling Overheating during Heat Waves. *Energy Build.* **2012**, *55*, 16–27. [CrossRef]
68. Leivo, V.; Prasauskas, T.; Du, L.; Turunen, M.; Kiviste, M.; Aaltonen, A.; Martuzevicius, D.; Haverinen-Shaughnessy, U. Indoor Thermal Environment, Air Exchange Rates, and Carbon Dioxide Concentrations before and after Energy Retrofits in Finnish and Lithuanian Multi-Family Buildings. *Sci. Total Environ.* **2018**, *621*, 398–406. [CrossRef] [PubMed]
69. Ministry of Health of the Republic of Lithuania. Lithuanian Hygiene Norm HN 42:2009 Microclimate in Residential and Public Buildings; Order No. V-1081, 29 December 2009. Available online: https://e-seimas.lrs.lt/portal/legalAct/lt/TAD/TAIS.362676 (accessed on 28 October 2026). (In Lithuanian)
70. International Energy Agency. *The Future of Cooling: Opportunities for Energy-Efficient Air Conditioning*; IEA: Paris, France, 2018. Available online: https://www.iea.org/reports/the-future-of-cooling (accessed on 26 October 2026).
71. United States Environmental Protection Agency. What Are Heat Islands? Available online: https://www.epa.gov/heatislands/what-are-heat-islands (accessed on 14 October 2026).
72. Giovannini, L.; Zardi, D.; de Franceschi, M. Characterization of the Thermal Structure inside an Urban Canyon: Field Measurements and Validation of a Simple Model. *J. Appl. Meteorol. Climatol.* **2013**, *52*, 64–81. [CrossRef]
73. Erell, E.; Pearlmutter, D.; Boneh, D.; Bar Kutiel, P. Effect of High-Albedo Materials on Pedestrian Heat Stress in Urban Street Canyons. *Urban Clim.* **2014**, *10*, 367–386. [CrossRef]
74. Schwaab, J.; Meier, R.; Mussetti, G.; Seneviratne, S.; Bürgi, C.; Davin, E.L. The Role of Urban Trees in Reducing Land Surface Temperatures in European Cities. *Nat. Commun.* **2021**, *12*, 6763. [CrossRef] [PubMed]

Disclaimer/Publisher's Note: The statements, opinions and data contained in all publications are solely those of the individual author(s) and contributor(s) and not of MDPI and/or the editor(s). MDPI and/or the editor(s) disclaim responsibility for any injury to people or property resulting from any ideas, methods, instructions or products referred to in the content.